Chapter 3

Hydroelectric System Models

Starting from general equations this chapter presents complete nonlinear models of a hydroelectric power plant, along with the simplifications that allow the obtaining of *new models*. On one hand, nonlinear models of hydroelectric power plants with or without surge tank effects are proposed -these models are useful in the design of new types of nonlinear controllers when large power variations are necessary. On the other hand, linearized models of hydroelectric power plants with surge tank effects are presented. In this case the models can be used when, for stability studies, a frequency response study is necessary.

Comprehensive tables are included where the new and the old models are classified. Besides, a practical method of calculating the mechanical power in steady state is shown. A time domain analysis of all models is presented along with a frequency response study of linearized models. The last part gives suggestions for modelling hydroelectric plants. The Appendix summarises the different models described in this chapter.

3.1 Preliminary Concepts

Authors in the bibliography use many kinds of notations to describe the variables and parameters. In order to study and compare the models, it is necessary to make use of uniform

the notation of the variables and parameters. This fact, subsequently, allows the description of different models of hydroelectric power plants. Table 3.1 lists and describes the parameters used in this Chapter, after making them uniform, and Table 3.2 presents the variables utilised after the same procedure is carried out.

PARAMETER	MEANING
$A_{(p,c,s)}$	Cross section area of a conduit in [m^2] (p: penstock, c: tunnel, s: surge tank).
$L_{(p,c)}$	Length of the conduit in [m] (p: penstock, c: tunnel).
a	Wave velocity in [m/s].
g	Acceleration due to gravity [m^2/s].
α	$\alpha = \rho \cdot g(1/\kappa + \phi/f \cdot E)$
ρ	Density of water [kg/m^3].
κ	Bulk modulus of compression of water [kg/($m \cdot s^2$].
ϕ	Internal conduit diameter [m].
f	Thickness of pipe wall [m].
E	Young's modulus of elasticity of pipe material.
$T_{\overline{w}}$	Water starting time at any load in [s].
$T_{WP,WC}$	Water starting time at rated or base load in [s] (WP: penstock, WC: tunnel).
C_s	Storage constant of surge tank in [s].
$T_{e,ep,ec}$	Elastic time in [s] (e: conduit, ep: penstock, ec: tunnel).
T_p	Pilot valve and servomotor time constant in [s].
T_g	Main servo time constant in [s].
T	Surge tank natural period in [s].
$f_{p1,p2,0}$	Head loss coefficients in [pu] (p1: penstock, p2: tunnel, 0: surge chamber orifice).
$\Phi_{p,c}$	Friction coefficient in [pu] (p: penstock, c: tunnel).
k_f	Head loss constant due to friction in [pu].
A_t	Turbine gain in [pu].
$z_{(p,c,n)}$	Hydraulic surge impedance of the conduit (p: penstock, c: tunnel, n: normalized).
D_1	Turbine damping in [pu/pu].

Table 3.1: List of parameters.

In Table 3.2 the superbar " - " indicates normalised values (expressed in [pu]).

VARIABLE	MEANING
$\overline{H}_{(t,r,l,l2,0,w)}$	Head in [pu] (t: turbine, r: riser of the surge tank, l: loss in penstock, l2: loss in tunnel, 0: reservoir, w: reservoir).
$\overline{U}_{(t,p,c,s,0,NL)}$	Velocity of the water in the conduit or flow in [pu] (t: turbine, p: penstock, c: tunnel, s: surge tank, 0: initial value, NL: no load).
$\overline{H}_{(tss,css)}$	Head in steady state [pu] (tss: turbine, css: tunnel).
$\overline{U}_{(tss,css)}$	Velocity or flow of the water in the conduit in steady state in [pu] (tss: turbine, css: tunnel).
$U \mid U_{(rated)}$	Velocity of the water in the conduit in [m/s] (rated: normalised)
$Q_{(base,\ rated)}$	Flow in the conduit in [m^3] (base, rated: turbine flow rate with gates fully open and head at the turbine equal to $H_{(base)}$).
$H \mid H_{(base)}$	Head in [m] (base: base value of head, i.e. the total available static head).
$\overline{G} \mid \Delta\overline{G}$	Gate opening in [pu]. / Deviation of the gate opening in [pu].
$\overline{P}_{mechanical} \mid \Delta\overline{P}_m$	Turbine mechanical power [pu]/Deviation of the mechanical power in [pu]
$\Delta\overline{\omega}$	Deviation of the rotor speed in [pu].

Table 3.2: List of variables.

In Figure 3.1 a complete layout of a hydraulic power plant is depicted. The main elements of this plant and some parameters are shown. On the other hand, Figure 3.2 shows the main variables of a hydroelectric power plant.

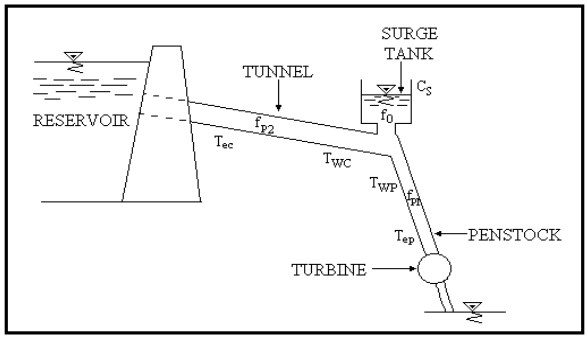

Figure 3.1: Plot of the distribution of parameters in a hydraulic power plant.

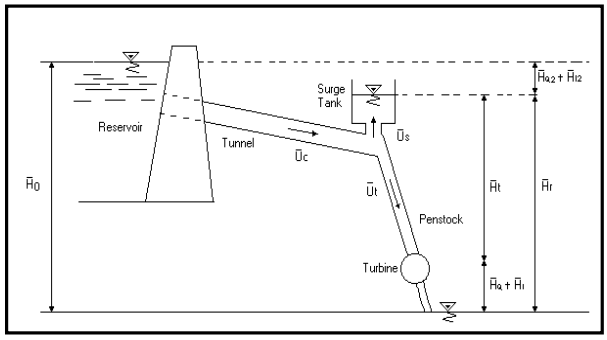

Figure 3.2: Plot of the distribution of heads and flows in a hydraulic power plant.

3.1.1 Definitions

The most significant parameters that govern a hydroelectric power plant are:

- Elastic time:

$$T_{e(p,c)} = L_{(p,c)} / a = L_{(p,c)} / \sqrt{g / \alpha}$$

- Hydraulic surge impedance of the conduit:

$$z_{(p,c)} = 1/\left(A_{(p,c)} \cdot \sqrt{g \cdot \alpha}\right)$$

The water starting time T_W is defined as the time required to accelerate the flow from zero to the rated (or base) flow ($Q_{(base)}$) under the base head ($H_{(base)}$) (Pegović *et al*, 1987).

- Water starting time in penstock:

$$T_{WP} = \frac{L_p}{A_p \cdot g} \cdot \frac{Q_{base}}{H_{base}} = z_p \cdot T_{ep}$$

- Water starting time in tunnel:

$$T_{WC} = \frac{L_c}{A_c \cdot g} \cdot \frac{Q_{base}}{H_{base}} = z_c \cdot T_{ec}$$

- Storage constant of surge tank:

$$C_s = \frac{A_s \cdot H_{base}}{Q_{base}}$$

- Surge tank natural period:

$$T = 2 \cdot \pi \cdot \sqrt{T_{WC} \cdot C_s}$$

- Relationship between flow and velocity of water in the conduit (tunnel or penstock):

$$Q = A \cdot U$$

- Relationship between the normalised flow and the normalised water velocity in the conduit (tunnel or penstock):

$$\frac{Q}{Q_{rated}} = \frac{A \cdot U}{A \cdot U_{rated}} \Rightarrow \overline{Q} = \overline{U}$$

3.1.2 System Dynamic Equations

The basic and general equations of the hydroelectric system dynamics (Kundur, 1994) are given by:

- Flow Equation (water velocity) in the penstock:

$$\overline{U}_t = \overline{G} \cdot \sqrt{\overline{H}_t} \qquad (3.\ 1)$$

- Mechanical Power Equations:

$$\overline{P}_{mechanical} = \overline{U} \cdot \overline{H} \tag{3. 2}$$

$$\overline{P}_{mechanical} = \left(\overline{U}_t - \overline{U}_{NL}\right) \cdot \overline{H}_t \tag{3. 3}$$

The difference between equations (3. 2) and (3. 3) is the term $\overline{U}_{NL}$ that considers the no load flow or the minimal flow needed to make the turbine deliver useful power.

- Newton's second law:

$$\frac{\partial U}{\partial t} = -g \cdot \frac{\partial H}{\partial x} \tag{3. 4}$$

- Continuity equation:

$$\frac{\partial U}{\partial x} = -\alpha \cdot \frac{\partial H}{\partial t} \tag{3. 5}$$

where x indicates the distance between two points and t is the time. The solutions of these equations (in per units) in the Laplace domain are given by:

$$\overline{U}_1 = \overline{U}_2 \cdot \cosh(T_e \cdot s) + 1/z_n \cdot \overline{H}_2 \cdot \sinh(T_e \cdot s) \tag{3. 6}$$

$$\overline{H}_2 = \overline{H}_1 \cdot \sec h(T_e \cdot s) - z_n \cdot \overline{U}_2 \cdot \tanh(T_e \cdot s) - k_f \cdot \overline{U}_2 \cdot \left|\overline{U}_2\right| \tag{3. 7}$$

The subscripts 1 and 2 refer to the conditions at the upstream and downstream ends of the conduit, respectively, e.g. when the surge tank-penstock-turbine hydraulic circuit is considered, the subscript 2 indicates downstream water (turbine) and the subscript 1 indicates upstream water (surge tank).

3.1.3 Linearized Equations

By linearizing the nonlinear relationships at an operating point, the flow in the penstock (3. 1) and the mechanical power (3. 2), become:

- Equation of the flow in the penstock (velocity of water)

$$\Delta\overline{U} = \frac{\partial\overline{U}}{\partial\overline{H}} \cdot \Delta\overline{H} + \frac{\partial\overline{U}}{\partial\overline{G}} \cdot \Delta\overline{G} = a_{11} \cdot \Delta\overline{H} + a_{13} \cdot \Delta\overline{G} \tag{3. 8}$$

- Equation of the mechanical power

$$\Delta\overline{P}_m = \frac{\partial\overline{P}_m}{\partial\overline{H}} \cdot \Delta\overline{H} + \frac{\partial\overline{P}_m}{\partial\overline{U}} \cdot \Delta\overline{U} = a_{21} \cdot \Delta\overline{H} + a_{23} \cdot \Delta\overline{U} \tag{3. 9}$$

The partial derivatives a_{11}, a_{13}, a_{21} and a_{23} depend on the kind of turbine and on the operating point. In Oldenburger and Donelson (1962) ideal values for the Francis turbine are $a_{11}= 0.5$, $a_{13}= 1$, $a_{21}= 1.5$ and $a_{23}= 1$.

3.1.4 Classification of the Models

The models can be classified in two basic groups:

- Nonlinear Models.
- Linearized Models.

3.2 Nonlinear Models

Nonlinear models of turbine hydraulic control systems are needed in those cases where large turbine velocity and power changes exist, for instance in isolated power stations, and, in cases when a load rejection happens and the electric system restoration follows a break-up.

In Figure 3.3 a block diagram of a hydroelectric system model is depicted, where the nonlinear dynamics (turbine and mechanical power) are included.

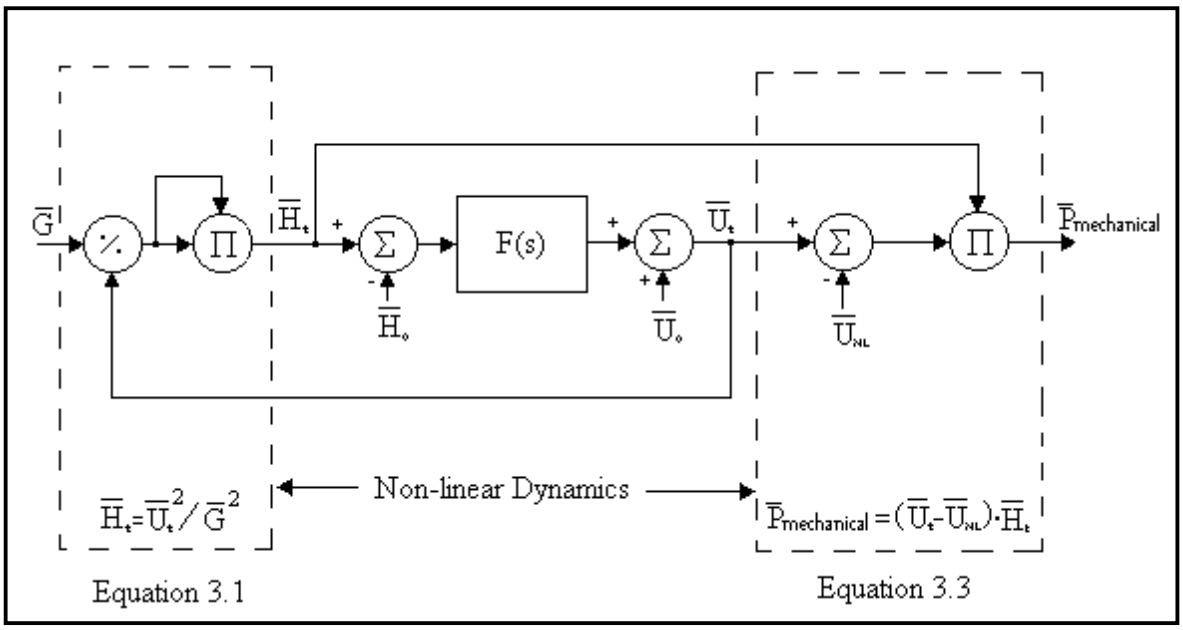

Figure 3.3: Block Diagram of the hydroelectric system used in the models of Kundur (1994).

Before describing different kinds of nonlinear models of hydroelectric systems, Table 3.3 presents a classification of these models: models *with surge tank effects* and models *with no surge tank effects*. Each one of these types has two more possibilities: the first considers elastic or non-elastic water columns, and the second takes into account the continuity equation as modified or non modified.

The associated number to each element of the table corresponds to the number of the Section of this Chapter where the model is described.

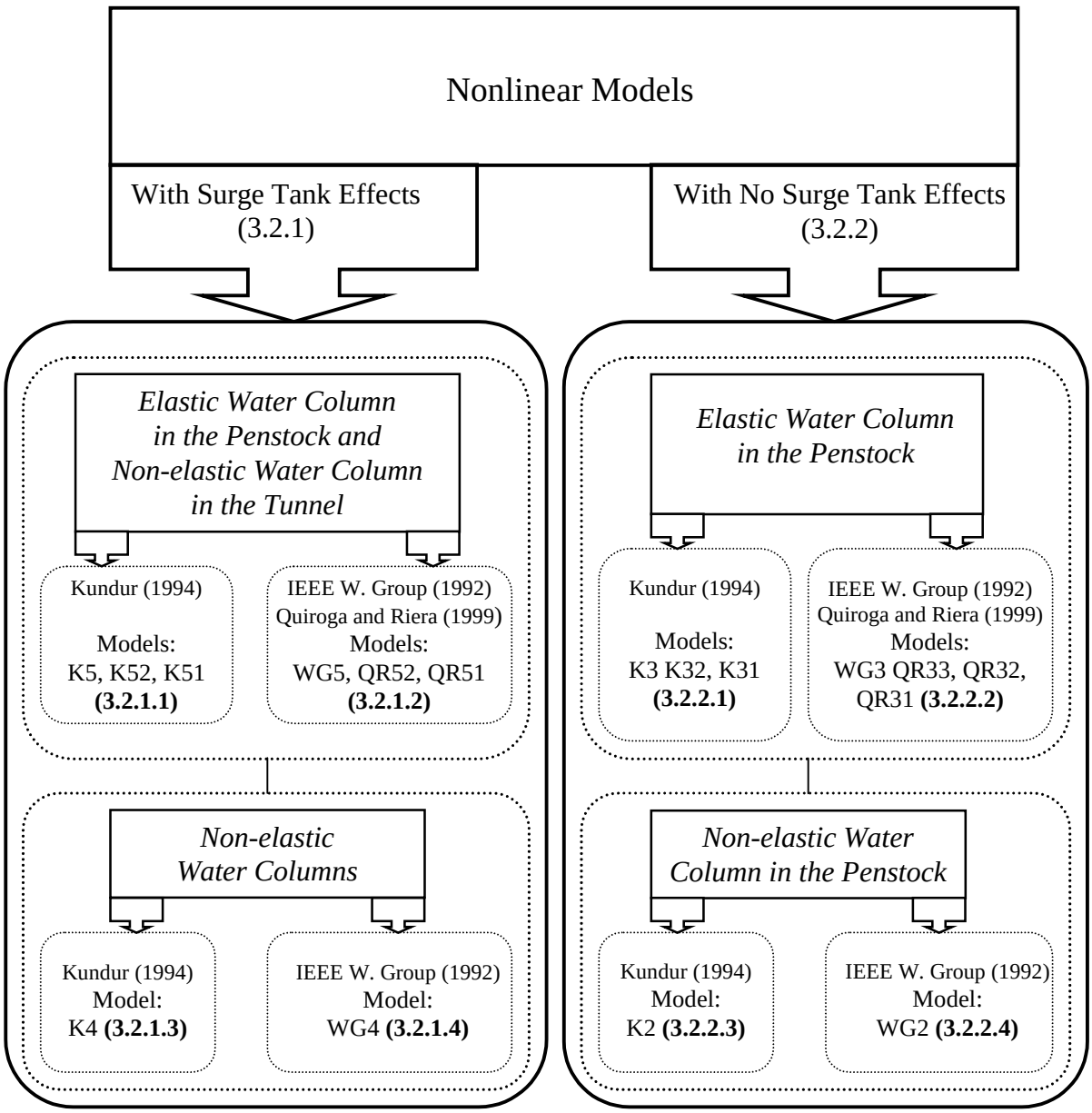

Table 3. 3: Table of nonlinear models.

3.2.1 Models with Surge Tank Effects

The main function of the surge tank is to hydraulically isolate the turbine from deviations generated in the head by transients in the conduits. By including the surge tank there appears an undulatory phenomenon whose time period is T. This Subsection presents those models that consider the surge tank effects.

3.2.1.1 Model with an elastic water column in the penstock and a non-elastic water column in the tunnel (Kundur, 1994) - Model K5, K51, K52

The model K5 is the most complete since it incorporates all relevant characteristics in a hydroelectric plant: it is a nonlinear model that includes surge tank effects, and considers an elastic water column in the penstock, a non-elastic water column in the tunnel, and the complete continuity equation.

Firstly, the relationship between the head and the flow in the turbine must be calculated. In this case equations (3. 6) and (3. 7) should be used in the following hydraulic circuits:

- Circuit 1: Reservoir-Tunnel-Surge Tank.
- Circuit 2: Surge Tank-Penstock-Turbine.

By combining conveniently both relationships, a transfer function is obtained, which connects the turbine flow and its head:

$$F(s) = \frac{\overline{U}_t - \overline{U}_0}{\overline{H}_t - \overline{H}_0} = -\frac{1 + \frac{G(s)}{z_p} \cdot \tanh(T_{ep} \cdot s)}{\Phi_p + G(s) + z_p \cdot \tanh(T_{ep} \cdot s)} \qquad (3.\ 10)$$

According to Oldenburger and Donelson (1962), G(s) is

$$G(s) = \frac{\overline{H}_0 - \overline{H}_s}{\overline{U}_p - \overline{U}_0} = \frac{\Phi_c + z_c \cdot \tanh(T_{ec} \cdot s)}{1 + s \cdot C_s \cdot \Phi_c + z_c \cdot \tanh(T_{ec} \cdot s) \cdot s \cdot C_s} \qquad (3.\ 11)$$

The hyperbolic tangent function is given by

$$\tanh(T_{ep} \cdot s) = \frac{1 - e^{-2 \cdot T_{ep} \cdot s}}{1 + e^{-2 \cdot T_{ep} \cdot s}} = \frac{s \cdot T_{ep} \cdot \prod_{n=1}^{n=\infty} \left(1 + \left(\frac{s \cdot T_{ep}}{n \cdot \pi}\right)^2\right)}{\prod_{n=1}^{n=\infty} \left(1 + \left(\frac{2 \cdot s \cdot T_{ep}}{(2 \cdot n - 1) \cdot \pi}\right)^2\right)} \qquad (3.\ 12)$$

Kundur (1994) considers for the hydraulic circuit reservoir-tunnel-surge tank the expansion with n=0, so $\tanh(T_{ec} \cdot s) \cong T_{ec} \cdot s$. The physical meaning is that the reservoir water level is considered constant. By replacing this result in (3. 11), G(s) becomes

$$G(s) = \frac{\overline{H}_s - \overline{H}_0}{\overline{U}_p - \overline{U}_0} = \frac{\Phi_c + s \cdot T_{WC}}{1 + s \cdot C_s \cdot \Phi_c + s^2 \cdot T_{WC} \cdot C_s} \qquad (3.\ 13)$$

The models K52 and K51 are obtained by considering in (3. 10) the approximations n=2 and n=1 of equation (3. 12). Finally, the models K5, K52 and K51 are completed by combining equations (3. 1), (3. 3), (3. 10) and (3. 13), as is it shown in Figure 3.3.

3.2.1.2 Model with an elastic water column in the penstock and a non-elastic water column in the tunnel (IEEE Working Group, 1992; Quiroga and Riera, 1999) - Models WG5, QR52, QR51

The solution of the continuity equation (3. 6) for these models is modified and is given by

$$\overline{U}_t = \overline{U}_c - \overline{U}_s \qquad (3.\ 14)$$

By applying this last equation in (3. 7), the dynamic equations of the hydraulic circuit 1 and circuit 2, can be expressed as follows.

- Dynamics of the Tunnel:

$$\overline{H}_r = 1.0 - \overline{H}_{l2} - \overline{H}_{Q2} \qquad (3.\ 15)$$

$$\overline{H}_{l2} = f_{p2} \cdot \overline{U}_c \cdot \left|\overline{U}_c\right| \qquad (3.\ 16)$$

$$\overline{H}_{Q2} = T_{WC} \cdot \frac{d\overline{U}_c}{dt} \qquad (3.\ 17)$$

- Dynamics of the Surge Tank:

$$\overline{H}_r = \frac{1}{C_s} \cdot \int \overline{U}_s \cdot dt - f_0 \cdot \overline{U}_s \cdot \left|\overline{U}_s\right| \qquad (3.\ 18)$$

- Dynamics of the Penstock:

$$\overline{H}_l = f_{p1} \cdot \overline{U}_t^{\,2} \qquad (3.\ 19)$$

$$\overline{H}_Q = z_p \cdot \tanh\left(T_{ep} \cdot s\right) \cdot \overline{U}_t \qquad (3.\ 20)$$

$$\overline{H}_t = \overline{H}_r - \overline{H}_l - z_p \cdot \tanh\left(T_{ep} \cdot s\right) \cdot \overline{U}_t = \overline{H}_r - \overline{H}_l - \overline{H}_Q \qquad (3.\ 21)$$

- Mechanical Power:

$$\overline{P}_{mechanical} = A_t \cdot \overline{H}_t \cdot \left(\overline{U}_t - \overline{U}_{NL}\right) - \overline{P}_{damping} \quad (3.\ 22)$$

$$\overline{P}_{damping} = D_1 \cdot \overline{G} \cdot \Delta\overline{\omega} \quad (3.\ 23)$$

The term $\overline{P}_{damping}$ represents the damping effect due to friction and it is proportional to the rotor speed deviation and to the gate opening. It is indispensable to include equation (3. 1) that represents the relation among the turbine flow, the turbine head and the gate opening. Figure 3.4 shows in detail a functional diagram with all the associated dynamics.

For the models QR52 and QR51 equations (3. 1), (3. 14) to (3. 20), (3. 22) and (3. 23) are valid; on the other hand if the approximations n=2,1 of (3. 12) in (3. 21) are considered, then

$$\overline{H}_t = \overline{H}_r - \overline{H}_l - z_p \cdot \tanh\left(T_{ep} \cdot s\right)_{n=1,2} \cdot \overline{U}_t \quad (3.\ 24)$$

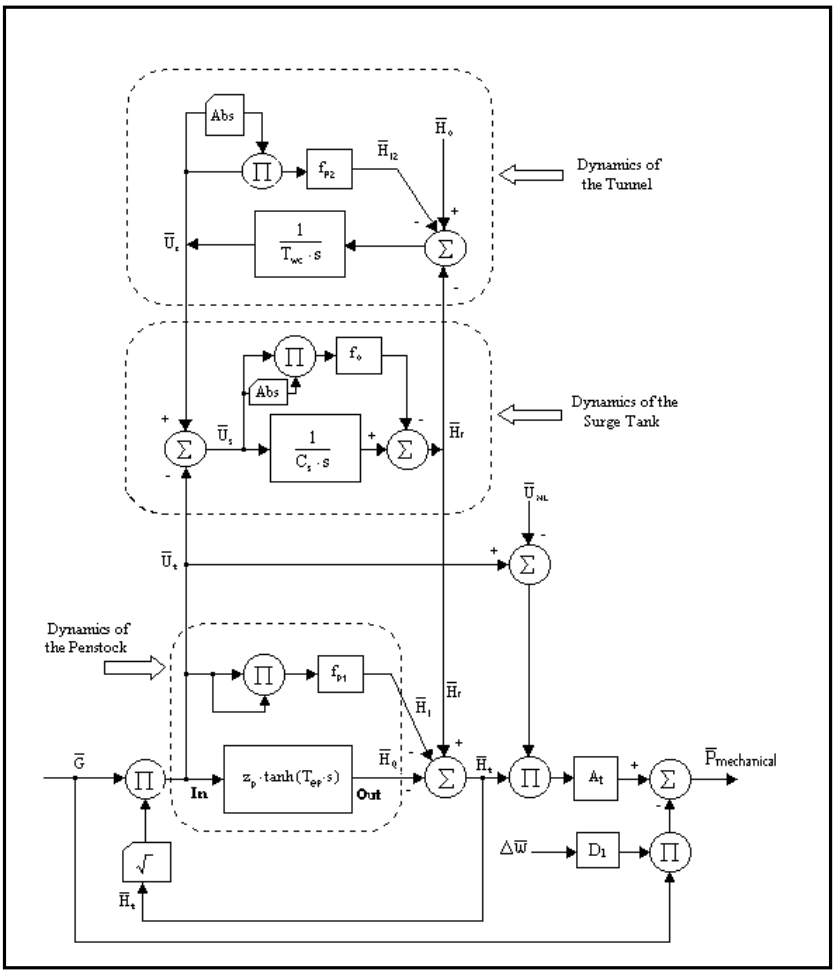

Figure 3.4: Functional diagram of model WG5 from the IEEE Working Group (1992) including associated dynamics.

3.2.1.3 Model with non-elastic water columns (Kundur, 1994) – Model K4

This model also considers the approximation $\tanh(T_{ec} \cdot s) \cong T_{ec} \cdot s$ - invariable water level of the reservoir - (Kundur, 1994). Since this model considers non-elastic water columns, these columns can be seen as rigid conduits, and the following result is deduced for the penstock: $\tanh(T_{ep} \cdot s) \cong T_{ep} \cdot s$ (IEEE Working Group, 1992). Hence, equation (3. 10) becomes

$$F(s) = \frac{\overline{U}_t - \overline{U}_0}{\overline{H}_t - \overline{H}_0} = -\frac{1 + \frac{G(s)}{z_p} \cdot T_{ep} \cdot s}{\Phi_p + G(s) + z_p \cdot T_{ep} \cdot s} \qquad (3.\ 25)$$

where G(s) for this equation comes from (3. 13).

Therefore, to obtain the complete model, as Figure 3.3 shows, equation (3. 25) must be combined with equations (3. 1) and (3. 3).

3.2.1.4 Model with non-elastic water columns (IEEE Working Group, 1992)–Model WG4

This model is based on equations (3. 14) to (3. 19), (3. 22) and (3. 23). Moreover, this model is obtained by considering the approximations: $\tanh(T_{ec} \cdot s) \cong T_{ec} \cdot s$ and $\tanh(T_{ep} \cdot s) \cong T_{ep} \cdot s$. The remaining equation of the dynamics of the penstock for this case is given by

$$\frac{d\overline{U}_t}{dt} = \frac{\overline{H}_r - \overline{H}_t - \overline{H}_l}{T_{WP}} \qquad (3.\ 26)$$

3.2.1.5 Comparisons between the models with an elastic water column in the penstock and a non-elastic water column in the tunnel (3.2.1.1 and 3.2.1.2)

The comparison between models with an elastic water column in the penstock and a non-elastic water column in the tunnel requires on one hand the analysis of the flow and head in the hydraulic circuit reservoir-tunnel-surge tank, and on the other hand the analysis of the equation of the dynamics of the surge tank.

Analysis of the Heads

The point of departure for model K5 is equation (3. 7), which is applied to the reservoir-tunnel-surge tank hydraulic circuit. The result is an equation that relates heads in this hydraulic circuit given by

$$\overline{H}_w{}' = \overline{H}_r + z_c \cdot \tanh(T_{ec} \cdot s) \cdot \overline{U}_c + \Phi_c \cdot \overline{U}_c$$

$$\overline{H}_w{}' = \overline{H}_r + T_{WC} \cdot (d\overline{U}_c / dt) + \overline{H}_{l2} = \overline{H}_r + \overline{H}_{Q2} + \overline{H}_{l2} \qquad (3.\ 27)$$

where

$$\overline{H}_w{}' = \overline{H}_w \cdot \sec h(T_{ec} \cdot s) \qquad (3.\ 28)$$

This means that the reservoir head $\overline{H}_w{}'$ is a function of s ($s = \sigma + j\omega$) and T_{ec}.

If the reservoir level is considered constant, as Subsection 3.2.1.3 shows, this means that the reservoir has considerably large dimensions and implies that $\tanh(T_{ec} \cdot s) \cong T_{ec} \cdot s$ and $\sec h(T_{ec} \cdot s) \cong 1$. Therefore, $\overline{H}_w{}' = \overline{H}_w$, and then

$$\overline{H}_w = \overline{H}_r + \overline{H}_{Q2} + \overline{H}_{l2} \qquad (3.\ 29)$$

In model WG5 the relationship of the heads in the reservoir-tunnel-surge tank hydraulic circuit is deduced from equation (3. 15), which is depicted in Figure 3.2, and can be reformulated as

$$\overline{H}_0 = \overline{H}_r + T_{WC} \cdot (d\overline{U}_c / dt) + \overline{H}_{l2} = \overline{H}_r + \overline{H}_{Q2} + \overline{H}_{l2} \qquad (3.\ 30)$$

where $\overline{H}_0 = \overline{H}_w = 1.0$. Hence, this last equation is *similar* to the equation of the heads of the model K5 (3. 29).

Analysis of the Flows

The comparison between the models K5 and WG5 requires, moreover, the analysis of the flows of the reservoir-tunnel-surge tank hydraulic circuit. By applying equation (3. 6) in model K5, then

$$\overline{U}_c = (\overline{U}_s + \overline{U}_t) \cdot \cosh(T_{ec} \cdot s) + 1/z_c \cdot \overline{H}_r \cdot \sinh(T_{ec} \cdot s) \qquad (3.\ 31)$$

According to the approximation $\tanh(T_{ec} \cdot s) \cong T_{ec} \cdot s$, whose significance is equivalent to $\cosh(T_{ec} \cdot s) \cong 1$ and $\operatorname{senh}(T_{ec} \cdot s) \cong T_{ec} \cdot s$, the continuity equation takes the following form

$$\overline{U}_c = \left(\overline{U}_s + \overline{U}_t\right) + 1/z_c \cdot \overline{H}_r \cdot (T_{ec} \cdot s) \qquad (3.\ 32)$$

In accordance with equation (3. 14), the model WG5 uses the following modified continuity equation (Figure 3.2)

$$\overline{U}_c = \overline{U}_s + \overline{U}_t$$

This equation implies that the impedance of the tunnel (z_c) is considered to be quite large, and in this dissertation is it called *the modified continuity equation* in order to differentiate it from the continuity equation, which is represented by equation (3. 31).

Analysis of the dynamic equation of the surge tank

In model K5 the equation of the surge tank without considering the riser (an element present in some surge tanks) has the following expression

$$\overline{H}_r = \frac{1}{C_s} \cdot \int \overline{U}_s \cdot dt \qquad (3.\ 33)$$

In model WG5 this dynamics is given by (3. 18). Therefore, the difference between both models is that K5 does not consider the surge chamber orifice head loss coefficient. Thus, the models consider different surge tanks.

3.2.1.6 Comparison between models with non-elastic water columns (3.2.1.3 and 3.2.1.4)

Analysis of the Heads

The analysis of the reservoir-tunnel-surge tank hydraulic circuit is coincident to the one presented in Subsection 3.2.1.5. The surge tank-penstock-turbine hydraulic circuit takes the approximation n=0 for the hyperbolic tangent function, or $\tanh(T_{ep} \cdot s) \cong T_{ep} \cdot s$ (non-elastic water column in the penstock). This also means that $\operatorname{sec h}(T_{ep} \cdot s) \cong 1$.

By applying equation (3. 7) to the surge tank-penstock-turbine hydraulic circuit,

$$\overline{H}_t = \overline{H}_r{}' - z_p \cdot \tanh\left(T_{ep} \cdot s\right) \cdot \overline{U}_t - \Phi_p \cdot \overline{U}_t$$

$$\overline{H}_t = \overline{H}_r{}' - \overline{H}_Q - \overline{H}_l$$

where $\overline{H}_r{}' = \overline{H}_r \cdot \operatorname{sec h}\left(T_{ec} \cdot s\right)$, so $\overline{H}_r{}' = \overline{H}_r$, and

$$\overline{H}_t = \overline{H}_r - \overline{H}_Q - \overline{H}_l \qquad (3.\ 34)$$

In model WG4 the relationship of the heads is deduced from equation (3. 21), which is *similar* to equation (3. 34), as can be seen in Figure 3.2. This means that there are not differences in heads between the models K4 and WG4.

3.2.2 Models with no Surge Tank Effects

In this part a second group of nonlinear models is presented. These are the models that do not consider surge tank effects.

3.2.2.1 Models with an elastic water column in the penstock (Kundur, 1994) – Models K3, K32, K31

To obtain the model K3, equations (3. 6) and (3. 7) are applied to the reservoir-penstock-turbine hydraulic circuit. By combining both equations, then

$$F(s) = \frac{\overline{U}_t - \overline{U}_0}{\overline{H}_t - \overline{H}_0} = -\frac{1}{\Phi_p + z_p \cdot \tanh\left(T_{ep} \cdot s\right)} \qquad (3.\ 35)$$

The models K32 and K31 are obtained by considering in (3. 35) the approximations n=2 and n=1 of (3. 12). Finally, the models K3, K32 and K31 are completed by combining equations (3. 1) and (3. 3), as can be seen in Figure 3.3.

3.2.2.2 Model with an elastic water column in the penstock (IEEE Working Group, 1992; Quiroga and Riera, 1999) – Model WG3, QR33, QR32, QR31

The model WG3 is obtained by combining equations: (3. 1), (3. 19), (3. 22), (3. 23) and the equation of the dynamic of the penstock, which for the present case is

$$\overline{H}_t = \left(\overline{H}_0 / \overline{H}_0\right) - \overline{H}_l - z_p \cdot \tanh\left(T_{ep} \cdot s\right) \cdot \overline{U}_t = 1.0 - \overline{H}_l - \overline{H}_Q \qquad (3.\ 36)$$

where

$$\overline{H}_Q = z_p \cdot \tanh\left(T_{ep} \cdot s\right) \cdot \overline{U}_t$$

For the models QR33, QR32 and QR31 equations (3. 1), (3. 19), (3. 22), (3. 23) are valid; on the other hand by considering the approximations n=2 and n=1 of the hyperbolic tangent (3. 12) in equation (3. 36), the dynamic of the penstock is given by

$$\overline{H}_t = 1.0 - \overline{H}_l - z_p \cdot \tanh\left(T_{ep} \cdot s\right)\Big|_{n=1,2} \cdot \overline{U}_t \qquad (3.\ 37)$$

3.2.2.3 Model with a non-elastic water column in the penstock (Kundur, 1994) – Model K2

This model is obtained by considering equation (3. 35) and the approximation of a non-elastic water column in penstock: $\tanh(T_{ep} \cdot s) \cong T_{ep} \cdot s$. Apart from this, the friction coefficient in the penstock is taken as $\Phi_p = 0$. The transfer function F(s) is, hence, given by

$$F(s) = \frac{\overline{U}_t - \overline{U}_0}{\overline{H}_t - \overline{H}_0} = -\frac{1}{T_{WP} \cdot s} \tag{3. 38}$$

To obtain the complete set of equations of this model it is necessary to combine this last equation with (3. 1) and (3. 3), as Figure 3.3 shows.

3.2.2.4 Model with a non-elastic water column in the penstock (IEEE Working Group, 1992) – Model WG2

This model is based on equations (3. 1), (3. 19), (3. 22), (3. 23) and an equation of the dynamics of the penstock, given by

$$\frac{d\overline{U}_t}{dt} = \frac{1.0 - \overline{H}_t - \overline{H}_l}{T_{WP}} \tag{3. 39}$$

3.2.2.5 Comparison between the models 3.2.2.1 and 3.2.2.2

Analysis of the Heads

Equation (3. 36) is taken as a point of departure, thus

$$\overline{H}_t = -z_p \cdot \tanh(T_{ep} \cdot s) \cdot \overline{U}_t - \overline{H}_l + 1.0 = -z_p \cdot \tanh(T_{ep} \cdot s) \cdot \overline{U}_t - f_{p1} \cdot \overline{U}_t + 1.0$$

$$\overline{H}_t - 1.0 = -z_p \cdot \tanh(T_{ep} \cdot s) \cdot \overline{U}_t - f_{p1} \cdot \overline{U}_t$$

$$\frac{\overline{U}_t}{\overline{H}_t - 1.0} = F(s) = -\frac{1}{z_p \cdot \tanh(T_{ep} \cdot s) + f_{p1}}$$

Therefore, a transfer function F(s) is found *similar* to the one obtained with equation (3. 35) in Kundur (1994). The distribution of the heads for a hydraulic plant without surge tank effects are shown in Figure 3. 5.

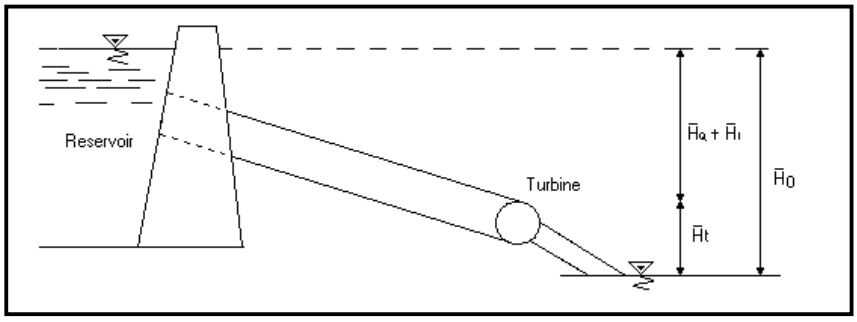

Figure 3. 5: Diagram of heads and flows distribution in models WG3, QR33, QR32, QR31 and WG2.

3.3 Linearized Models

These models are obtained by combining the linearized equation of the mechanical power (3. 2) and the linearized equation of the flow (3. 1). These models are useful in cases of small signal stability as well as frequency response studies (IEEE Working Group, 1992; Kundur, 1994). The linearized models are classified in Table 3.4.

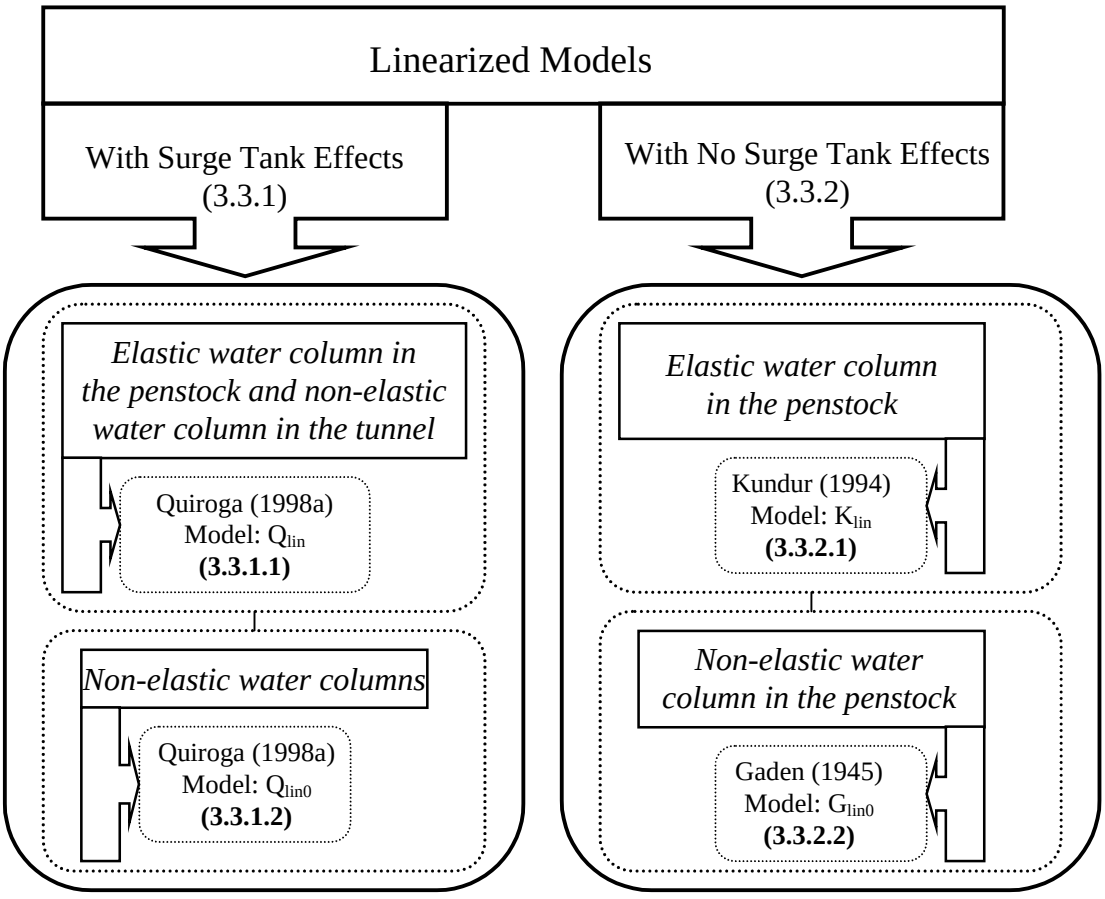

Table 3. 4: Table of the linearized models.

3.3.1 Models with Surge Tank Effects

3.3.1.1 Model with an elastic water column in the penstock and a non-elastic water column in the tunnel (Quiroga, 1998a) –Model Q_{lin}

This model is based on the combination of the flow in the penstock (3. 8), the mechanical power (3. 9) (both linearized at an operating point) and the transfer functions F(s) (3. 10) and G(s) (3. 13).

$$\frac{\Delta\overline{P}_m}{\Delta\overline{G}} = \frac{1-\Phi_p - z_p\cdot\tanh\left(T_{ep}\cdot s\right)+\dfrac{G(s)}{z_p}\cdot\tanh\left(T_{ep}\cdot s\right)-G(s)}{1+0.5\cdot\Phi_p+0.5\cdot z_p\cdot T_{ep}\cdot s+0.5\cdot G(s)+\dfrac{G(s)}{z_p}\cdot\tanh\left(T_{ep}\cdot s\right)} \qquad (3.\ 40)$$

This model may be interesting when a frequency response study is necessary, in particular, when stability studies are required.

3.3.1.2 Model with non-elastic water columns (Quiroga, 1998a) – Model Q_{lin0}

The model Q_{lin0} is obtained from the model Q_{lin} by considering the approximation n=0 for the hyperbolic tangent, which means to consider a non-elastic water column in the penstock.

By using equations: (3. 8), (3. 9), (3. 13) and (3. 25), where non-elastic water columns are considered, the resulting transfer function is

$$\frac{\Delta\overline{P}_m}{\Delta\overline{G}} = \frac{1-\Phi_p - z_p\cdot T_{ep}\cdot s+\dfrac{G(s)}{z_p}\cdot T_{ep}\cdot s-G(s)}{1+0.5\cdot\Phi_p+0.5\cdot z_p\cdot T_{ep}\cdot s+0.5\cdot G(s)+\dfrac{G(s)}{z_p}\cdot T_{ep}\cdot s} \qquad (3.\ 41)$$

3.3.2 Models with no Surge Tank Effects

3.3.2.1 Model with an elastic water column in the penstock (Kundur, 1994) – Model K_{lin}

This model is obtained by combining equations (3. 8), (3. 9) and (3. 35) where an elastic water in penstock column is considered:

$$\frac{\Delta\overline{P}_m}{\Delta\overline{G}} = \frac{1-\Phi_p - z_p\cdot\tanh\left(T_{ep}\cdot s\right)}{1+0.5\cdot\Phi_p+0.5\cdot z_p\cdot\tanh\left(T_{ep}\cdot s\right)} \qquad (3.\ 42)$$

3.3.2.2 Models with a non-elastic water column in the penstock (Gaden, 1945) – Model G_{lin0}

These models are based on equations (3. 8), (3. 9) and (3. 38). Here the transfer function F(s) considers a non-elastic water column in the penstock and the penstock head loss coefficient equal to zero. The transfer function that relates the mechanical power with the gate opening for the ideal turbine case has the following expression

$$\frac{\Delta\overline{P}_m}{\Delta\overline{G}} = \frac{1 - z_p \cdot T_{ep} \cdot s}{1 + 0.5 \cdot z_p \cdot T_{ep} \cdot s} = \frac{1 - T_{WP} \cdot s}{1 + 0.5 \cdot T_{WP} \cdot s} \tag{3. 43}$$

This transfer function has been used for fifty years since the simplicity of representing a hydroelectric plant with no surge tank effects by a transfer function with one pole and one zero.

In general, for the non ideal turbine case, the transfer function conserves its shape of one pole and one zero, the difference are the coefficients that here represent partial differentiation at an operating point, and coincide with the coefficients in equations (3. 8) and (3. 9) (Ramey and Skooglund, 1970).

$$\frac{\Delta\overline{P}_m}{\Delta\overline{G}} = a_{23} \cdot \frac{1 + \left(a_{11} - a_{13} \cdot a_{21} / a_{23}\right) \cdot T_{\varpi} \cdot s}{1 + a_{11} \cdot T_{\varpi} \cdot s} \tag{3. 44}$$

3.4 Conclusions of the Presented Models

Two ways of classifying the hydroelectric models into groups have been presented. The first considers the nonlinear models, since two of their equations are nonlinear: the mechanical power; and the relationship among the turbine flow, the turbine head and the gate opening. The second takes into account the linearized models, where the above mentioned equations are linearized at an operating point. Both groups can also be divided into models with and without surge tank effects. Apart from that, both sub-groups consider the following possibilities: 1) an elastic water column in the penstock and a non-elastic water column in the tunnel, and 2) non-elastic water columns.

To simplify some models, two approximations are considered. The first supposes the reservoir level as invariable, or a very large reservoir, which mathematically can be written as $\tanh(T_{ec} \cdot s) \cong T_{ec} \cdot s$. The second considers non-elastic water column in the penstock (rigid conduit), which mathematically is equivalent to $\tanh(T_{ep} \cdot s) \cong T_{ep} \cdot s$.

The nonlinear models allow the representation of the behaviour of hydroelectric power plants, in an accurate manner, and can be used at every operating point without modifying the parameters: T_{WP}, T_{WC} or C_s.

On the other hand, when linearized models are considered, these parameters must be adjusted at the operating point. Furthermore, linearized models allow the studying of models from the frequency response viewpoint, and thus facilitating the control system stability study or small-signal stability study.

3.5 Static Analysis

Analysis of the steady state behaviour of some representative models is proposed in this section. The main objective is to determine the value in steady state of the main process variables (flow, head and gate opening) and, also, to calculate the mechanical power that the hydroelectric plant generates in the steady state.

Kundur (1994) uses in his developments the variable $\overline{U}_0$, which allows the formulation of the models as a transfer function represented by means of F(s) (equations (3. 10) or (3. 25)). Therefore, it is useful to determine $\overline{U}_0$ when the models of Kundur (1994) are considered. First, the flow of the turbine in steady state $\overline{U}_{tss}$ is computed and then the variable $\overline{U}_0$ is calculated. There are two ways of calculating this last variable: the first corresponds to the equation of the dynamics of the penstock (according to Kundur (1994)), which is taken as an initial step. The second is derived from the comparison between the models of Kundur (1994) and the IEEE Working Group (1992).

Furthermore, it is included in this Section a manner of presenting the calculation of the minimal flow needed by the turbine to overcome the problem of friction, or the no load flow ($\overline{U}_{NL}$).

3.5.1 Determination of the Flow of the Turbine in Steady State

3.5.1.1 Calculation of $\overline{U}_{tss}$ for a nonlinear model with surge tank effects

For simplicity in the following explanation the nonlinear model WG4 (Section 3.2.1.4) with surge tank effects and non-elastic water columns is considered. However, the same results are obtained if the nonlinear models WG5, QR52 or QR51, with surge tank effects and an elastic water column in the penstock and a non-elastic column in the tunnel (Section 3.2.1.2) are used instead.

Equations that describe this model come from equations: (3. 14) to (3. 19), (3. 22), (3. 23) and (3. 26). If these equations are written in a convenient manner, then the following system is obtained:

$$\begin{cases} \dfrac{d\overline{U}_t}{dt} = \dfrac{1}{T_{WP}} \cdot \overline{H}_r - \left(\dfrac{1}{T_{WP} \cdot \overline{G}^2} + \dfrac{f_{p1}}{T_{WP}} \right) \cdot \overline{U}_t^2 \\ \dfrac{d\overline{H}_r}{dt} = \dfrac{\overline{U}_c}{C_s} - \dfrac{\overline{U}_t}{C_s} \\ \dfrac{d\overline{U}_c}{dt} = \dfrac{1}{T_{WC}} - \dfrac{\overline{H}_r}{T_{WC}} - \dfrac{f_{p2}}{T_{WC}} \cdot \overline{U}_c^2 \end{cases} \tag{3. 45}$$

Since in steady state the variations of the state variables $\overline{U}_t$, $\overline{H}_r$ and $\overline{U}_c$ with respect to time are zero, then

$$\begin{cases} 0 = \dfrac{1}{T_{WP}} \cdot \overline{H}_{rss} - \left(\dfrac{1}{T_{WP} \cdot \overline{G}^2} + \dfrac{f_{p1}}{T_{WP}} \right) \cdot \overline{U}_{tss}^2 \\ 0 = \dfrac{\overline{U}_{css}}{C_s} - \dfrac{\overline{U}_{tss}}{C_s} \\ 0 = \dfrac{1}{T_{WC}} - \dfrac{\overline{H}_{rss}}{T_{WC}} - \dfrac{f_{p2}}{T_{WC}} \cdot \overline{U}_{css}^2 \end{cases}$$

Operating conveniently, the following equations are obtained

$$\begin{cases} \overline{H}_{rss} = \left(\dfrac{1}{\overline{G}^2} + f_{p1} \right) \cdot \overline{U}_{tss}^2 \\ \overline{U}_{tss}^2 = \dfrac{1}{f_{p2}} - \dfrac{\overline{H}_{rss}}{f_{p2}} \\ \overline{U}_{tss} = \overline{U}_{css} \end{cases}$$

The solutions of this system are:

$$\overline{H}_{rss} = \frac{f_{p1} + \frac{1}{\overline{G}^2}}{f_{p2} + f_{p1} + \frac{1}{\overline{G}^2}} \tag{3. 46}$$

$$\overline{U}_{tss} = \overline{U}_{css} = \sqrt{\frac{1}{f_{p2}} \cdot \left(1 - \frac{f_{p1} + \frac{1}{\overline{G}^2}}{f_{p2} + f_{p1} + \frac{1}{\overline{G}^2}}\right)} = \sqrt{\frac{\overline{G}^2}{1 + \overline{G}^2 \cdot (f_{p1} + f_{p2})}} \tag{3. 47}$$

Hence, the values of the state variables in steady state are a function of the friction coefficients of the tunnel and the penstock, i.e. the tunnel and the penstock head loss coefficients, and the gate opening.

3.5.1.2 Deduction of $\overline{U}_{tss}$ for a nonlinear model with no surge tank effects

The deduction can be made in a similar way by using the model WG2 with no surge tank effects and a non-elastic water column in the penstock (Section 3.2.2.4). From the equations (3. 1), (3. 19) and (3. 39) the following expression is obtained

$$\frac{d\overline{U}_t}{dt} = \frac{1}{T_{WP}} \cdot \left(1 - \frac{\overline{U}_t^2}{\overline{G}^2} - f_{p1} \cdot \overline{U}_t^2\right)$$

In steady state the turbine flow variation is zero. Hence, the expression of the flow in steady state can be written as

$$\overline{U}_{tss} = \sqrt{\frac{1}{\frac{1}{\overline{G}^2} + f_{p1}}} \tag{3. 48}$$

3.5.1.3 Determination of $\overline{U}_0$ used in the models of Kundur (1994)

The reasoning starts from equation (3. 7) for the surge tank-penstock-turbine hydraulic circuit, and the following expression is obtained

$$\overline{H}_t - \overline{H}_0 = (\overline{H}_r - \overline{H}_0) \cdot \sec h(T_{ep} \cdot s) - (z_p \cdot \tanh(T_{ep} \cdot s) + \Phi_p) \cdot (\overline{U}_t - \overline{U}_0)$$

This equation in steady state becomes

$$\overline{H}_{tss} = \overline{H}_{rss} - \Phi_p \cdot \left(\overline{U}_{tss} - \overline{U}_0\right) \tag{3. 49}$$

Equation (3. 7) written for the reservoir-tunnel-surge tank hydraulic circuit is

$$\overline{H}_r - \overline{H}_0 = \left(\overline{H}_w - \overline{H}_0\right) \cdot \sec h(T_{ec} \cdot s) - \left(z_c \cdot \tanh(T_{ec} \cdot s) + \Phi_c\right) \cdot \left(\overline{U}_c - \overline{U}_0\right)$$

By considering $\overline{H}_0 = \overline{H}_w = 1.0$, then

$$\overline{H}_r - \overline{H}_0 = -\left(z_c \cdot \tanh(T_{ec} \cdot s) + \Phi_c\right) \cdot \left(\overline{U}_c - \overline{U}_0\right)$$

For steady state this last expression is

$$\overline{H}_{rss} = \overline{H}_0 - \Phi_c \cdot \left(\overline{U}_{tss} - \overline{U}_0\right) \tag{3. 50}$$

Replacing (3. 50) in (3. 49) and recalling that $\overline{H}_{tss} = \overline{U}_{tss}^2 / \overline{G}^2$, then

$$\overline{U}_0 = \overline{U}_{tss} + \frac{\dfrac{\overline{U}_{tss}^2}{\overline{G}^2} - \overline{H}_0}{\Phi_p + \Phi_c} \tag{3. 51}$$

Therefore, when the models from Kundur (1994) are utilised, the variable $\overline{U}_0$ must be adjusted for each value of the gate opening ($\overline{G}$).

In Figure 3.6 the variable $\overline{U}_0$ in steady state for two hydroelectric power stations, whose values are shown in Table 3.5, is plotted. This figure shows a parabolic shape since it is a function of the square of the gate opening.

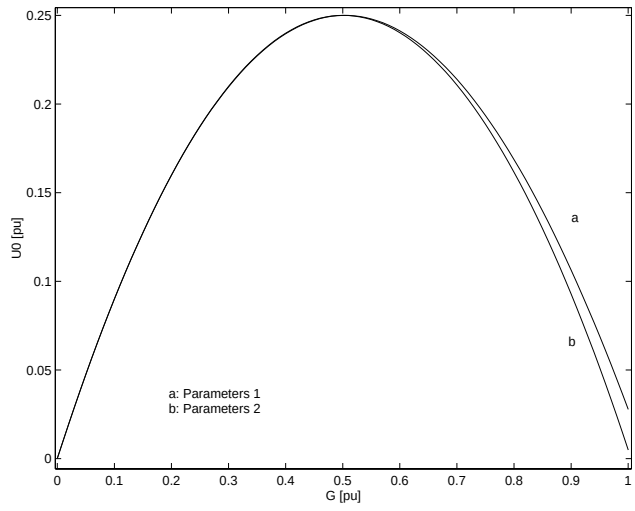

Figure 3.6: Plot of $\overline{U}_0$ in function of the variable $\overline{G}$ for two hydroelectric power stations.

3.5.1.4 Determination of $\overline{U}_0$ by using the comparison between equations

In this section the initial flow $\overline{U}_0$ is obtained from the dynamics of the tunnel, which is described by IEEE Working Group (1992), although Kundur (1994) presents a similar dynamics of the tunnel, as it is explained bellow:

- The dynamics of the tunnel for the case of Kundur is obtained by writing equation (3. 7) for the reservoir-tunnel-surge tank hydraulic circuit. Thus,

$$\overline{H}_r - \overline{H}_0 = \left(\overline{H}_w - \overline{H}_0\right)\cdot \sec h(T_{ec}\cdot s) - \left(z_c \cdot \tanh(T_{ec}\cdot s) + \Phi_c\right)\cdot\left(\overline{U}_c - \overline{U}_0\right)$$

Once again, $\overline{H}_0 = \overline{H}_w = 1.0$ is considered. By taking the approximation: $\tanh(T_{ec}\cdot s) \cong T_{ec}\cdot s$, and recalling that $T_{WC} = T_{ec}\cdot z_c$, then

$$\overline{H}_r = \overline{H}_0 - \left((T_{WC}\cdot s) + \Phi_c\right)\cdot\left(\overline{U}_c - \overline{U}_0\right) \qquad (3.\ 52)$$

- Combining the equations (3. 15) and (3. 16), the following expression is obtained

$$\overline{H}_r = 1.0 - T_{WC}\cdot s\cdot\overline{U}_c - f_{p2}\cdot\overline{U}_c\cdot\left|\overline{U}_c\right| \qquad (3.\ 53)$$

At this point, it is supposed that the friction coefficient of the tunnel (Φ_c) is equal to the tunnel head loss coefficient (f_{p2}). This supposition is replaced in equation (3. 53).

Valuing (3. 52) and (3. 53) for steady state and equalling them, hence

$$\left(\overline{U}_{css} - \overline{U}_0\right) = \overline{U}_{css}^2$$

In addition, as $\overline{U}_{css} = \overline{U}_{tss}$, the following expression for the flow can be inferred:

$$\overline{U}_0 = \overline{U}_{tss} - \overline{U}_{tss}^2 \qquad (3.\ 54)$$

3.5.1.5 Verification of supposition made in 3.5.1.4.

In the preceding Section a first consideration has been proposed where the friction coefficient of the tunnel (Φ_c) was supposed equal to the tunnel head loss coefficient (f_{p2}). At

this point a second consideration is needed to make the comparison between the models of IEEE Working Group (1992) and Kundur (1994). This second consideration supposes that the friction coefficient of the penstock (Φ_p) is equal to the penstock head loss coefficient (f_{p1}).

The next demonstration has the objective to show that these suppositions are completely valid. The first step is to equal equations (3. 54) and (3. 51):

$$\overline{U}_{tss} + \frac{\frac{\overline{U}_{tss}^2}{\overline{G}^2} - \overline{H}_0}{\Phi_p + \Phi_c} = \overline{U}_{tss} - \overline{U}_{tss}^2$$

operating mathematically the last expression, gives

$$\overline{U}_{tss} = \sqrt{\frac{\overline{H}_0}{\frac{1}{\overline{G}^2} + \Phi_p + \Phi_c}}$$

equalling (3. 47) and the previous expression, hence

$$\frac{\overline{H}_0}{\frac{1}{\overline{G}^2} + \Phi_p + \Phi_c} = \frac{\overline{G}^2}{1 + \overline{G}^2 \cdot (f_{p1} + f_{p2})}$$

operating conveniently, then

$$\Phi_p - f_{p1} = f_{p2} - \Phi_c$$

From this expression a possible and reasonable solution is to consider $f_{p1} = \Phi_p$ and $f_{p2} = \Phi_c$.

❑

3.5.2 Determination of the Mechanical Power

3.5.2.1 Calculations for nonlinear models with and with no surge tank effects

- When the surge tank effects are considered, the expression of the mechanical power is given by equation (3. 22). Then the following expression for steady state is obtained

$$\overline{P}_{mecss} = A_t \cdot \left(\overline{U}_{tss} - \overline{U}_{NL}\right) \cdot \overline{H}_{tss} = A_t \cdot \left(\overline{U}_{tss} - \overline{U}_{NL}\right) \cdot \frac{\overline{U}_{tss}^2}{\overline{G}^2} \qquad (3.\ 55)$$

Note that for steady state the term $D_1 \cdot \overline{G} \cdot \Delta\overline{\omega}$ is equal to zero.

If equation (3. 47) is replaced in (3. 55), then

$$\overline{P}_{mecss} = \frac{A_t \cdot \overline{G}}{\left(1 + \overline{G}^2 \cdot \left(\Phi_c + \Phi_p\right)\right)^{3/2}} - \frac{A_t \cdot \overline{U}_{NL}}{1 + \overline{G}^2 \cdot \left(\Phi_c + \Phi_p\right)} \qquad (3.\ 56)$$

For a specific power station the values of Φ_c, Φ_p, A_t and $\overline{U}_{NL}$ are constants; therefore, the mechanical power varies as a function of the gate opening $\overline{G}$.

- Following the same procedure for a model with *no* surge tank effects the equation (3. 48) is replaced in equation (3. 55), then

$$\overline{P}_{mecss} = \frac{A_t \cdot \overline{G}}{\left(1 + \overline{G}^2 \cdot \Phi_p\right)^{3/2}} - \frac{A_t \cdot \overline{U}_{NL}}{1 + \overline{G}^2 \cdot \Phi_p} \qquad (3.\ 57)$$

Considering a power station with no surge tank effects, clearly means that the plant has no tunnel and the tunnel friction coefficient of the tunnel (Φ_c) disappears from the expression of the mechanical power in steady state.

3.5.2.2 Calculations for a linearized model with and with no surge effects

For the case of a model with surge tank effects, equation (3. 41) may be taken as an initial step, and by applying the final value theorem, the following expression can be obtained for the steady state

$$\overline{P}_{mecss} = \lim_{s \to 0} \left(s \cdot \frac{1 - \Phi_p - z_p \cdot T_{ep} \cdot s + \frac{F_1(s)}{z_p} \cdot T_{ep} \cdot s - F_1(s)}{1 + 0.5 \cdot \Phi_p + 0.5 \cdot z_p \cdot T_{ep} \cdot s + 0.5 \cdot F_1(s) + \frac{F_1(s)}{z_p} \cdot T_{ep} \cdot s} \cdot \frac{\overline{G}}{s} \right)$$

$$\overline{P}_{mecss} = \frac{1 - \Phi_p - \Phi_c}{1 + 0.5 \cdot \Phi_p + 0.5 \cdot \Phi_c} \cdot \overline{G} \qquad (3.\ 58\ )$$

In the case of model with no surge tank effects it is necessary to take, as a starting point, the equation (3. 42). Applying the final value theorem, then

$$\overline{P}_{mecss} = \lim_{s\to 0}\left(s \cdot \frac{1-\Phi_p - z_p \cdot \tanh\left(T_{ep}\cdot s\right)}{1+0.5\cdot\Phi_p + 0.5\cdot z_p \cdot \tanh\left(T_{ep}\cdot s\right)} \cdot \frac{\overline{G}}{s} \right) = \frac{1-\Phi_p}{1+0.5\cdot\Phi_p}\cdot\overline{G} \qquad (3.\ 59)$$

which evidently is a particular case of the previous one. In Figure 3.7 is plotted the mechanical power value in steady sate for two hydroelectric plants whose parameters are in Table 3.5.

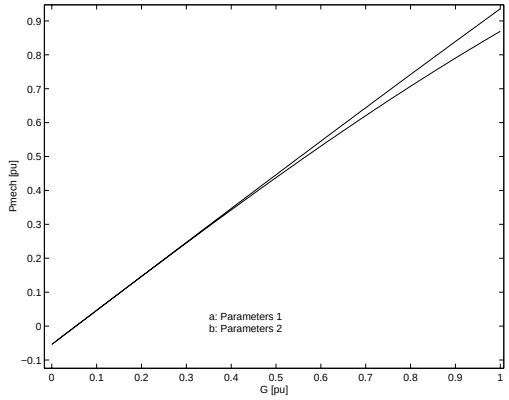

Figure 3.7: Mechanical power generated by the turbine in hydroelectric plants with surge tank effects as function of $\overline{G}$.

3.5.2.3 Calculation of the gate opening ($\overline{G}$) for $\overline{P}_{mecss} = 0$

It is important to determine the minimum value of the gate opening that the turbine needs to generate net power. Two possible cases are analysed:

- Case 1: Plant with surge tank effects.

If $\overline{P}_{mecss} = 0$ is considered in equation (3. 56), then

$$\overline{G}_{(P_{mecss}=0)} = \frac{A_t \cdot \overline{U}_{NL}}{\left(1-\overline{U}_{NL}^2 \cdot \left(\Phi_c + \Phi_p\right)\right)^{1/2}}$$

The expression $\overline{U}_{NL}^2 \cdot \left(\Phi_c + \Phi_p\right)$ takes a very small value for real parameters of hydroelectric plants, hence, the minimum value of the gate opening may be approximated by

$$\overline{G}_{(P_{mecss}=0)} \cong A_t \cdot \overline{U}_{NL} \tag{3. 60}$$

- Case 2: Plant with no surge tank effects.

In the same way in equation (3. 57) is considered $\overline{P}_{mecss} = 0$, then

$$\overline{G}_{(P_{mecss}=0)} = \frac{A_t \cdot \overline{U}_{NL}}{\left(1 - \overline{U}_{NL}^2 \cdot \Phi_p\right)^{1/2}} \tag{3. 61}$$

In this case the expression $\overline{U}_{NL}^2 \cdot \Phi_p$ takes a small value for real power plants, and it can be affirmed that $\overline{G}_{(P_{mecss}=0)} \cong A_t \cdot \overline{U}_{NL}$.

Parameters	IEEE W. Group (1) *With STE* IEEE Working Group (1992)	Appalachia (2) *With STE* Oldenburger and Donelson (1962)	Susqueda (3) *With STE* Quiroga (1999)	Blenheim-Gilboa 3 (4) *With no STE* Hannet *et al.* (1994)	St Lawrence 32 (5) *With no STE* Hannet *et al.* (1994)	Niagara 1 (6) *With no STE* Hannet *et al.* (1994)
T_{WP} [s]	1.77	1	0.82	1.72	0.39	0.9
T_{WC} [s]	5.79	52	9.15	-	-	-
C_s [s]	138.22	900	170.7	-	-	-
T_{ep} [s]	0.42	0.25	0.208	0.06246*	0.0205	0.0328*
f_{p1} [pu]	0.0138	0.03	0.01	0.01*	0.01*	0.01*
f_{p2} [pu]	0.046	0.12	0.05	-	-	-
f_0 [pu]	0.1854	0	0	-	-	-
A_t [pu]	1.004	1	1.67	1.4	1.65	1.17
$\overline{U}_{NL}$ [pu]	0.0538	0.0538	0.13	0.185	0.184	0.094
T_g [s]	0.5	0.5	0.5	0.67	0.5	0.1
z_p	4.187	4	3.95	27.5376	19.024	27.439
T [s]	178	1370	248	-	-	-

Table 3.5: Parameters for different power plants. (* Means estimated parameters)

3.6 Time Domain Analysis of Models

In this section a time domain analysis for all models presented in Sections 3.2 and 3.3 is proposed. The simulation toolbox SIMULINK of the MATLAB software is utilised to obtain the time response of nonlinear and linearized models. For a good comprehension of the dynamic study, the analysis is divided into four subsections.

3.6.1 Nonlinear Models with Surge Tank Effects

This set of models may also be divided into two groups. On one hand the models of the IEEE Working Group (1992) and the derived models of Quiroga and Riera (1999); on the other hand the models of Kundur (1994) and their derived models.

3.6.1.1 Models WG4, QR51, QR52, WG5

In Figure 3.4 the functional diagram of model WG5 is depicted and Figure 3.8 presents the block used for the calculation of the hyperbolic tangent, which is a part of the penstock dynamic used in this nonlinear model with surge tank effects and elastic water column in the penstock and non-elastic water column in the tunnel.

Figure 3.9 represents the block used in the calculation of the hyperbolic tangent. Here the hyperbolic tangent is approximated by equation (3. 12) (models WG4, QR51, QR52).

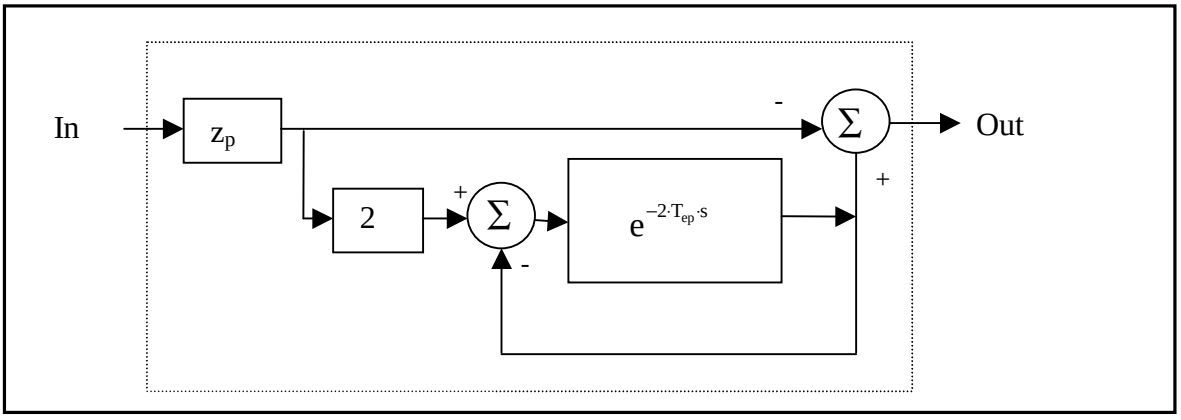

Figure 3.8: Representation of the block used for the calculation of the hyperbolic tangent (model WG5).

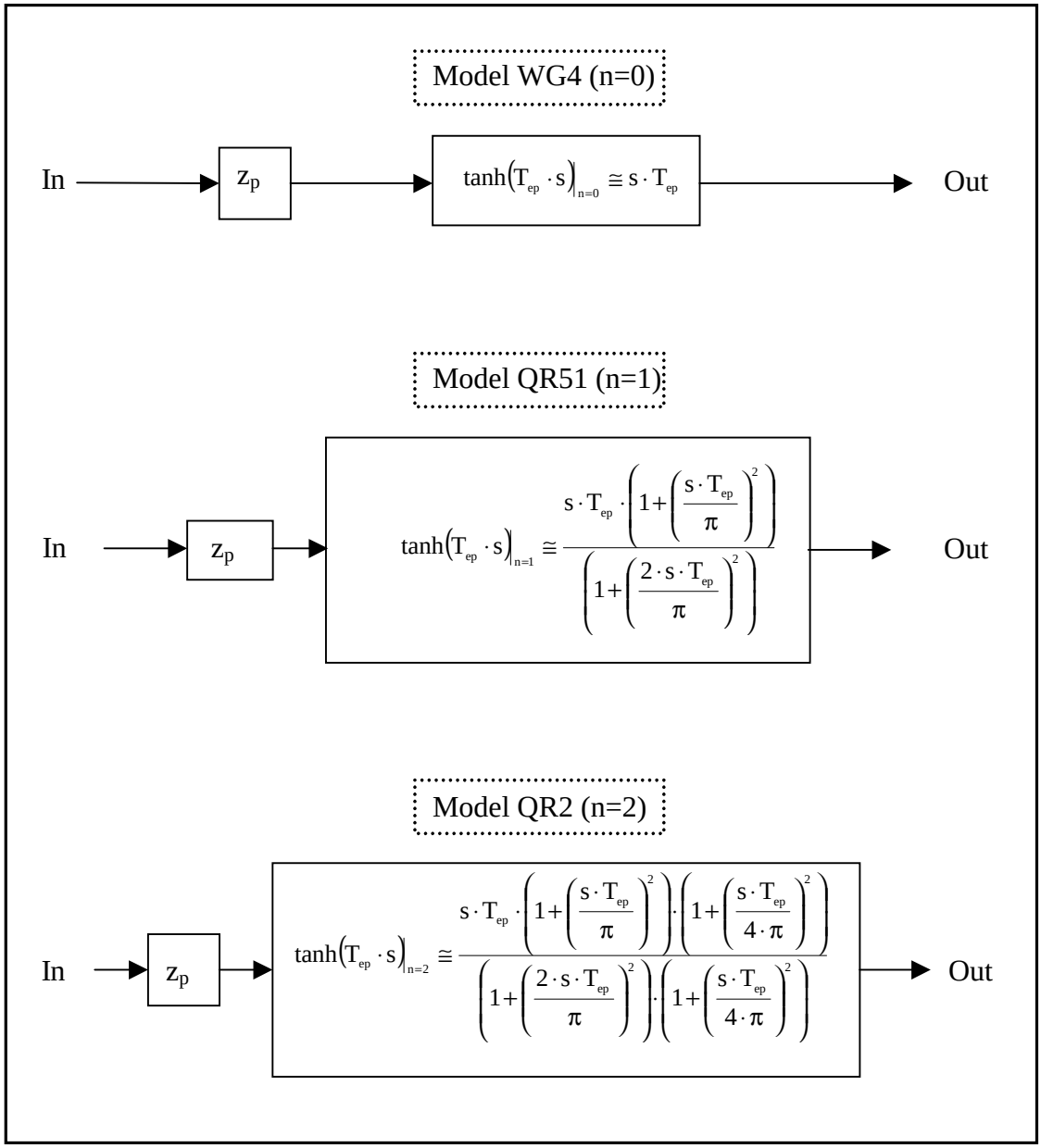

Figure 3.9: Representation of the block that can be used for the calculation of the hyperbolic tangent function in the models WG4 (n=0), QR51 (n=1) and QR52 (n=2).

Several lumped-parameters approximations of the hyperbolic tangent are considered:

- For n=0, hyperbolic tangent has the following expression

$$\tanh\left(T_{ep}\cdot s\right)\cong s\cdot T_{ep}$$

- For n=1:

$$\tanh\left(T_{ep}\cdot s\right)\cong\frac{s\cdot T_{ep}\cdot\left(1+\left(\frac{s\cdot T_{ep}}{\pi}\right)^2\right)}{\left(1+\left(\frac{2\cdot s\cdot T_{ep}}{\pi}\right)^2\right)}$$

- For n=2:

$$\tanh\left(T_{ep}\cdot s\right)\cong\frac{s\cdot T_{ep}\cdot\left(1+\left(\frac{s\cdot T_{ep}}{\pi}\right)^2\right)\cdot\left(1+\left(\frac{s\cdot T_{ep}}{2\cdot\pi}\right)^2\right)}{\left(1+\left(\frac{2\cdot s\cdot T_{ep}}{\pi}\right)^2\right)\cdot\left(1+\left(\frac{2\cdot s\cdot T_{ep}}{3\cdot\pi}\right)^2\right)}$$

- For n=3:

$$\tanh\left(T_{ep}\cdot s\right)\cong\frac{s\cdot T_{ep}\cdot\left(1+\left(\frac{s\cdot T_{ep}}{\pi}\right)^2\right)\cdot\left(1+\left(\frac{s\cdot T_{ep}}{2\cdot\pi}\right)^2\right)\cdot\left(1+\left(\frac{5\cdot s\cdot T_{ep}}{3\cdot\pi}\right)^2\right)}{\left(1+\left(\frac{2\cdot s\cdot T_{ep}}{\pi}\right)^2\right)\cdot\left(1+\left(\frac{2\cdot s\cdot T_{ep}}{3\cdot\pi}\right)^2\right)\cdot\left(1+\left(\frac{2\cdot s\cdot T_{ep}}{5\cdot\pi}\right)^2\right)}$$

Figures 3.10 and 3.11 show the responses after applying a step function of a ten per cent on the gate opening for different nonlinear models with surge tank effects. The models from (IEEE Working Group, 1992) these are: WG5 and WG4 and the derived models from the lumped-parameters approximations of the hyperbolic tangent (Quiroga and Riera, 1999) equation (3. 24). In both figures the response of the turbine mechanical power is depicted.

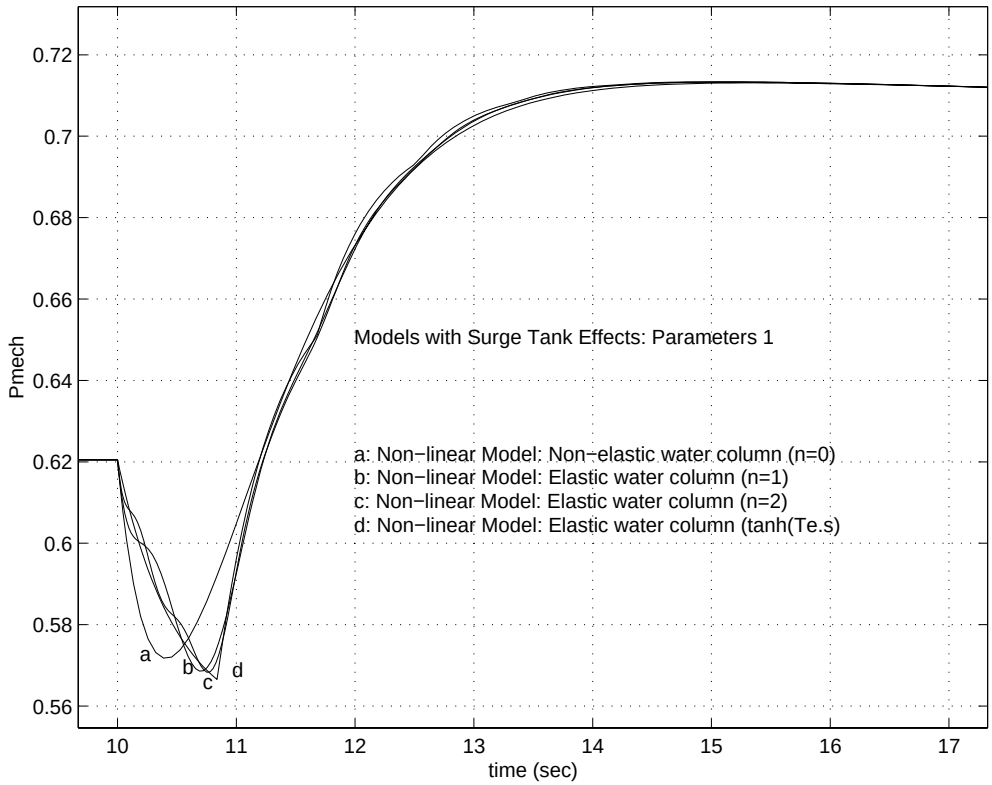

Figure 3.10: Comparison among the models WG4, QR51, QR52 and WG5, detail.

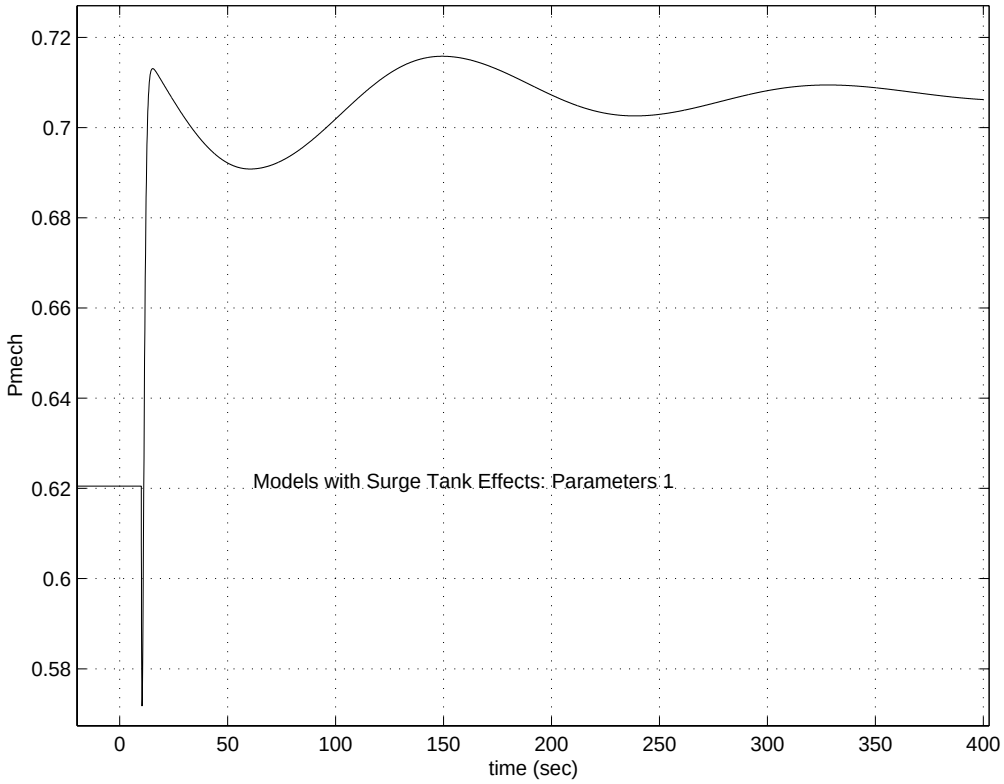

Figure 3.11: Comparison among the models WG4, QR51, QR52 and WG5.

Figure 3.10 shows the non-minimal phase behaviour of the models of hydroelectric systems. The model WG4 (non-elastic water columns, graphic a) presents a phase lag compared to the group formed by the models QR51 (graphic b), QR52 (graphic c), and the model that considers the exact value of the hyperbolic tangent WG5 (graphic d).

It is important to note the oscillation period caused by the surge tank, which is presented in Figure 3.11. The period (T) of this oscillation depends on the physical characteristics of the hydroelectric system such as the cross sections of the tunnel and the surge tank, and the length of the tunnel, and is given by

$$T = 2 \cdot \pi \cdot \sqrt{\frac{A_s \cdot L_T}{g \cdot A_T}} = 2 \cdot \pi \cdot \sqrt{T_{WC} \cdot C_s} \qquad (3.\ 62)$$

3.6.1.2 Models K4, K51, K52

To simulate the models of Kundur 1994 and models derived from them, the hyperbolic tangent must be approximated; therefore, equation (3. 10) is turned into

$$F(s) = \frac{\overline{U}_t - \overline{U}_0}{\overline{H}_t - \overline{H}_0} = -\frac{1 + \frac{G(s)}{z_p} \cdot \tanh(T_{ep} \cdot s)\Big|_{n=0,1,2}}{\Phi_p + G(s) + z_p \cdot \tanh(T_{ep} \cdot s)\Big|_{n=0,1,2}}$$

Figure 3.12 shows a block diagram that is used for the temporal dynamic study of the models of Kundur (1994) and his derived models.

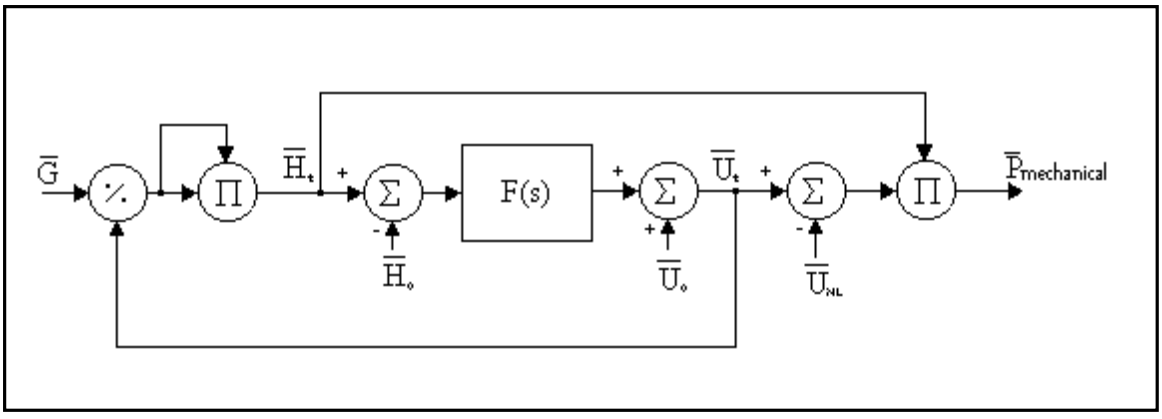

Figure 3.12: Block diagram for the models of Kundur (1994) and his derived models.

In Figures 3.13 and 3.14 the simulation results for the models K4, K51 and K52 (Kundur, 1994) by using the approximations of the hyperbolic tangent are presented. The variable $\overline{U}_0$ is adjusted according to the value of the gate opening (equation (3. 51)).

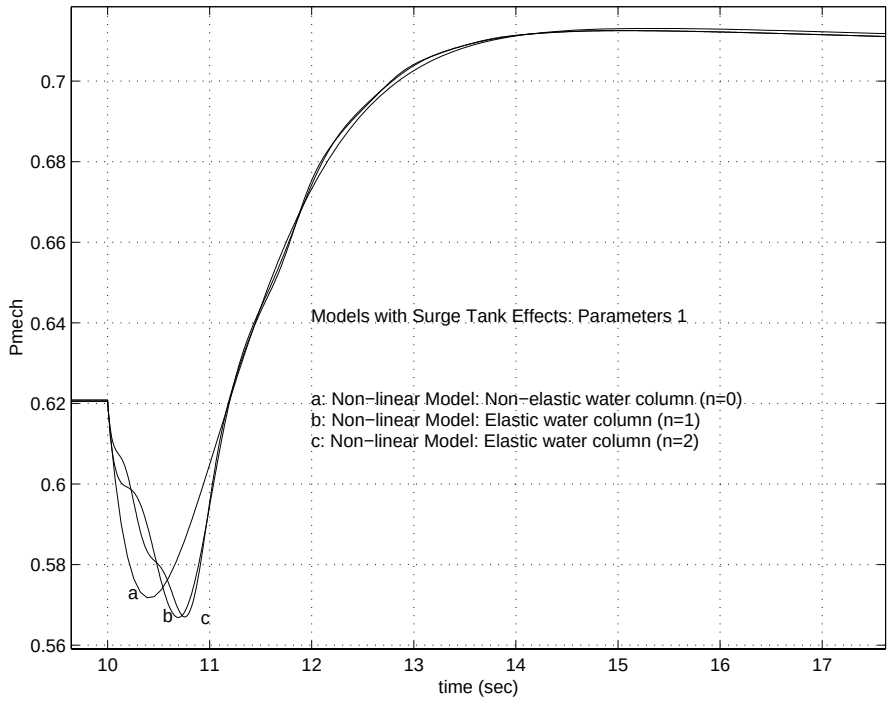

Figure 3.13: Comparison among the models K4, K51 and K52, detail.

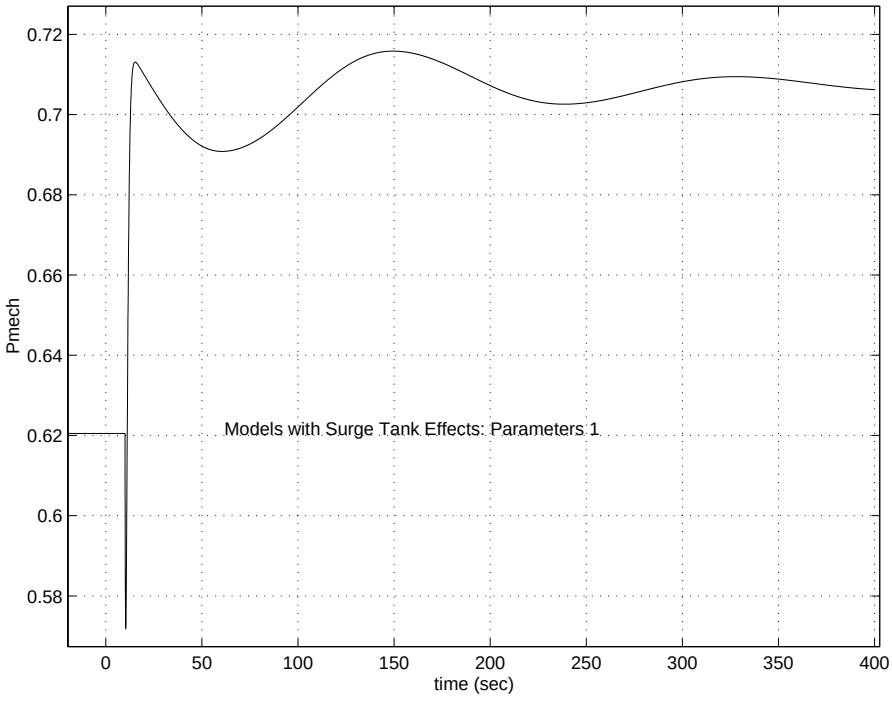

Figure 3.14: Comparison among the models K4, K51 and K52.

Graphics a, b and c of Figure 3.13 correspond to graphics a, b and c of Figure 3.10. Both figures are obtained, according to the parameters of Table 3.5, by simulating nonlinear models with surge tank effects. The steady state is reached when the oscillation of period T is completely damped, as Figure 3.14 shows.

3.6.2 Linearized Models with Surge Tank Effects

The time starting constants of the tunnel and penstock (T_{WC} and T_{WP}) for the linearized models must be adjusted according to the variation of the gate opening ($\overline{G}$). In these cases, according to Kundur (1994), the constant $T_{\overline{w}}$ is used, and is calculated by

$$T_{\overline{w}} = \left(\frac{L}{g \cdot A} \right) \cdot \frac{Q_0}{H_0}$$

It is known that in a nominal operating point (subscript 0)

$$\overline{Q}_0 = \overline{G}_0 \cdot \sqrt{\overline{H}_0} \quad \Rightarrow \quad \frac{Q_0}{Q_{base}} = \overline{G}_0 \cdot \sqrt{\frac{H_0}{H_{base}}}$$

replacing Q_0 into the first expression

$$T_{\overline{w}} = \left(\frac{L}{g \cdot A} \right) \cdot \overline{G}_0 \frac{Q_{base} \cdot \sqrt{\frac{H_0}{H_{base}}}}{H_0}$$

as $H_0 \cong H_{base}$

$$T_{\overline{w}} = \left(\frac{L}{g \cdot A} \right) \cdot \overline{G}_0 \cdot \frac{Q_{base}}{H_{base}} \cong T_W \cdot \overline{G}_0 \qquad (3.\ 63)$$

The surge constant C_s must also be adjusted according to the following expression

$$C_{\overline{S}} = \frac{A_s \cdot H_{base}}{Q_{base} \cdot \overline{G}_0} = \frac{C_s}{\overline{G}_0} \qquad (3.\ 64)$$

Equation (3. 40) is used to simulate these models, where the hyperbolic tangent is approximated for n=0,1,2:

$$\frac{\Delta\overline{P}_m}{\Delta\overline{G}} = \frac{1-\Phi_p - z_p\cdot\tanh\left(T_{ep}\cdot s\right)\Big|_{n=0,1,2} + \dfrac{G(s)}{z_p}\cdot\tanh\left(T_{ep}\cdot s\right)\Big|_{n=0,1,2} - G(s)}{1+0.5\cdot\Phi_p + 0.5\cdot z_p\cdot T_{ep}\cdot s + 0.5\cdot G(s) + \dfrac{G(s)}{z_p}\cdot\tanh\left(T_{ep}\cdot s\right)\Big|_{n=0,1,2}}$$

3.6.2.1 Model Q_{lin0}

Figure 3.15 shows the response obtained when the gate opening varies a one per cent. The behaviour is similar to that produced by a nonlinear model with surge tank effects and non-elastic water columns WG4 and K4, see graphic a from Figures 3.10 and 3.13

Figure 3.16 shows the way the steady state is reached after a damping oscillation whose period is T.

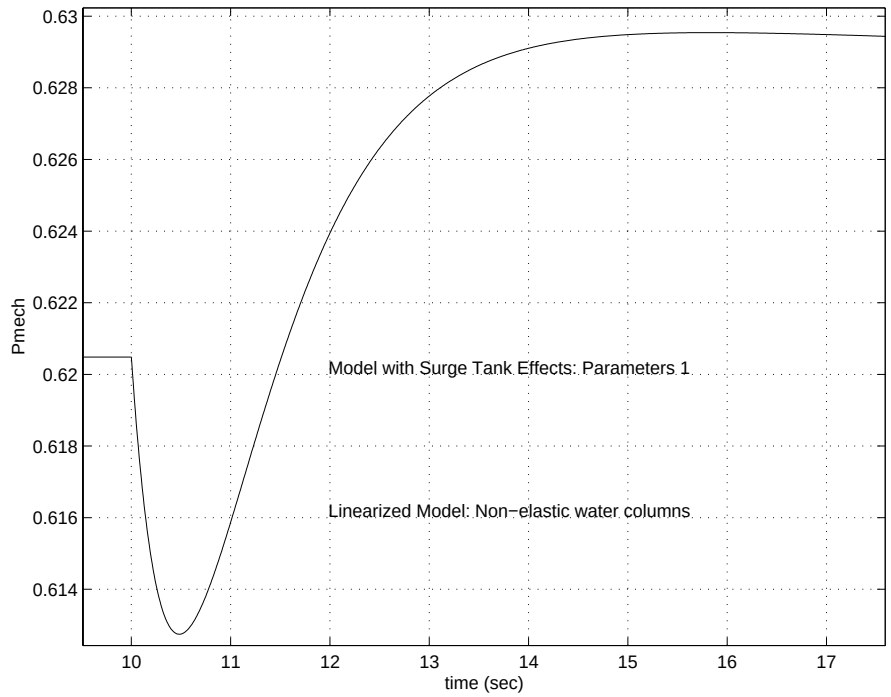

Figure 3.15: Simulation of the linearized model Q_{lin0}, for a variation of 0.01 [pu] in the gate opening, detail.

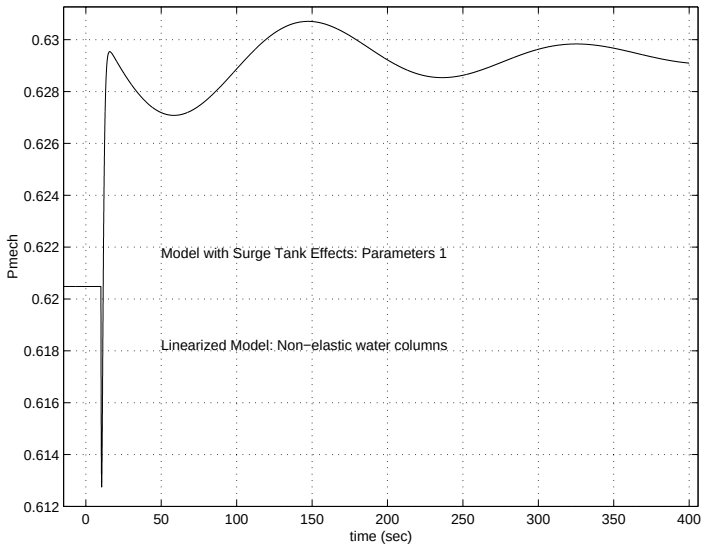

Figure 3.16: Simulation of the linearized model Q_{lin0}, for a variation of 0.01 [pu] in the gate opening.

3.6.3 Nonlinear Models with no Surge Tank Effects

The following figure represents a functional scheme of model WG3 with no surge tank effects according to IEEE Working Group (1992).

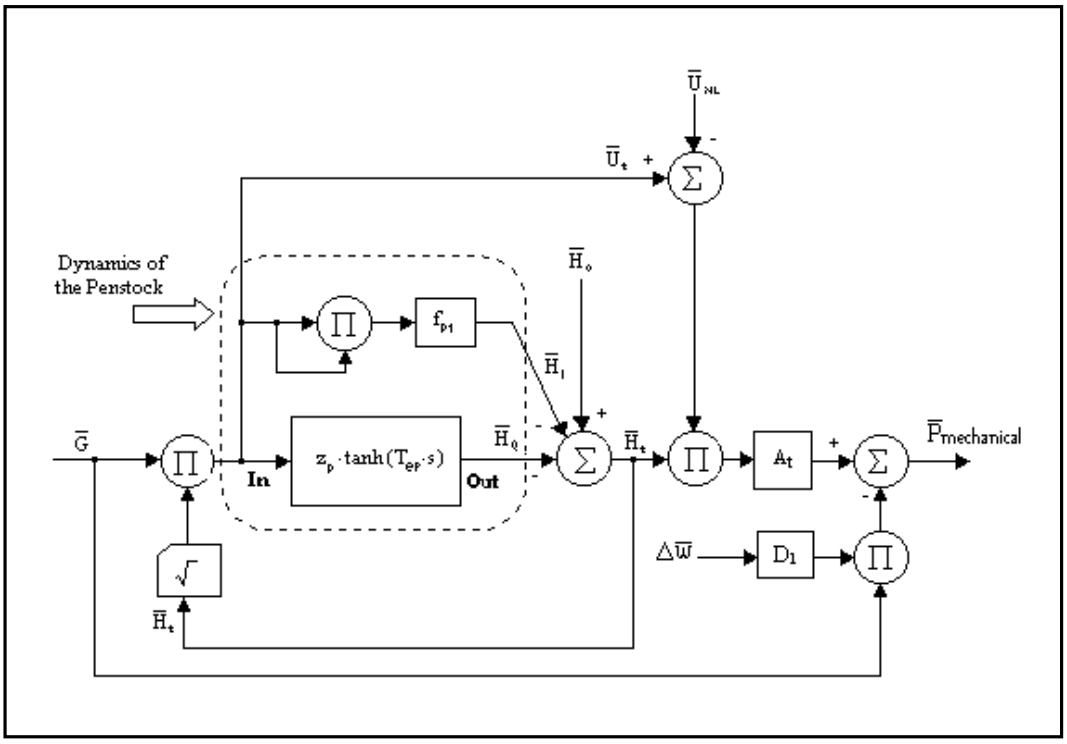

Figure 3.17: Functional scheme of a model WG3 from (IEEE Working Group, 1992).

On one hand, the “In-Out” block of Figure 3.8 is used to simulate the model WG3. On the other hand, the blocks of Figure 3.9 are utilised to simulate the models: WG2, QR31, and QR32.

3.6.3.1 Models WG2, QR31, QR32, QR33

Using the approximation of the hyperbolic tangent function, the equation of the turbine head is expressed as

$$\overline{H}_t = 1 - \overline{H}_l - z_p \cdot \tanh\left(T_{ep} \cdot s\right)\Big|_{n=0,1,2,3} \cdot \overline{U}_t \qquad (3.\ 65)$$

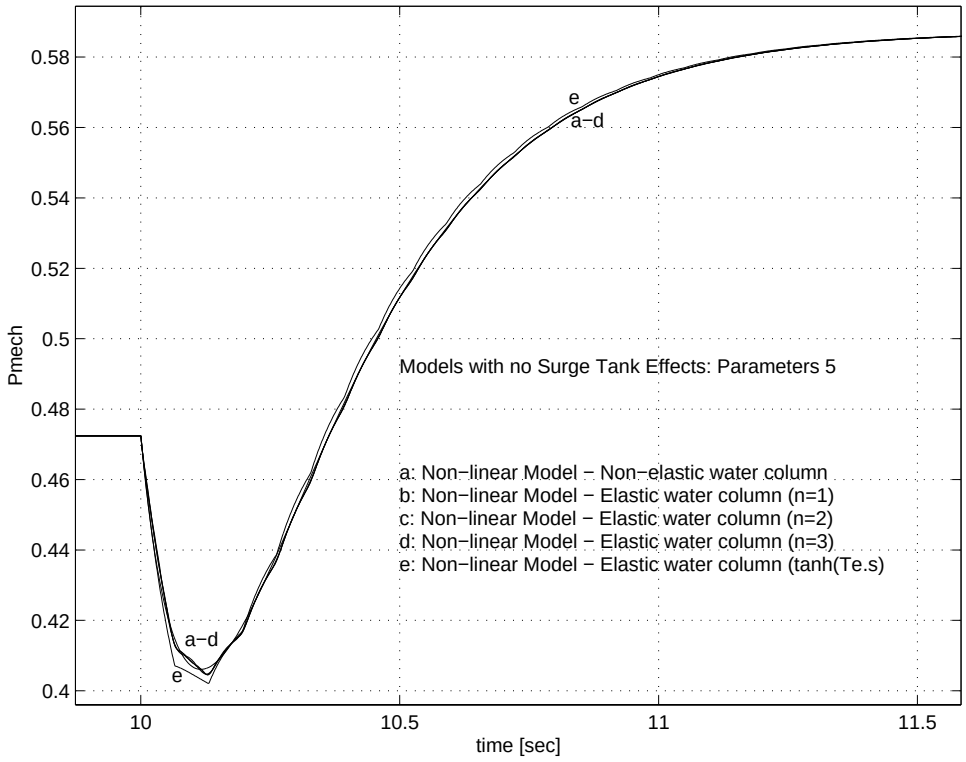

Figure 3.18: Comparison among the models WG2, QR31, QR32, QR33 and WG3.

Figure 3.18 depicts the simulation results for models with no surge tank effects, which correspond to the hydroelectric plant of St. Lawrence 32 and whose parameters are shown in Table 3.5. A slightly different behaviour during the transient can be seen, which does not appear in hydroelectric plants with surge tank effects. This difference can also be observed in the model that considers a non-elastic water column in the penstock (WG2, graphic a).

When surge tank effects are not considered; there is no phase lag between the responses of the models with an elastic or a non-elastic water column in the penstock.

It can be seen, moreover, that simulations for n=0,1,2,3 approximations have a similar behaviour. There appears a slight difference for the response of the model WG3 (graphic e).

3.6.3.2 Models K2, K31, K32

These models are based on equation (3. 35), where the hyperbolic tangent function is approximated for n=0,1,2. Therefore, the transfer function becomes

$$F(s) = \frac{\overline{U}_t - \overline{U}_0}{\overline{H}_t - \overline{H}_0} = -\frac{1}{\Phi_p + z_p \cdot \tanh(T_{ep} \cdot s)\Big|_{n=0,1,2}}$$

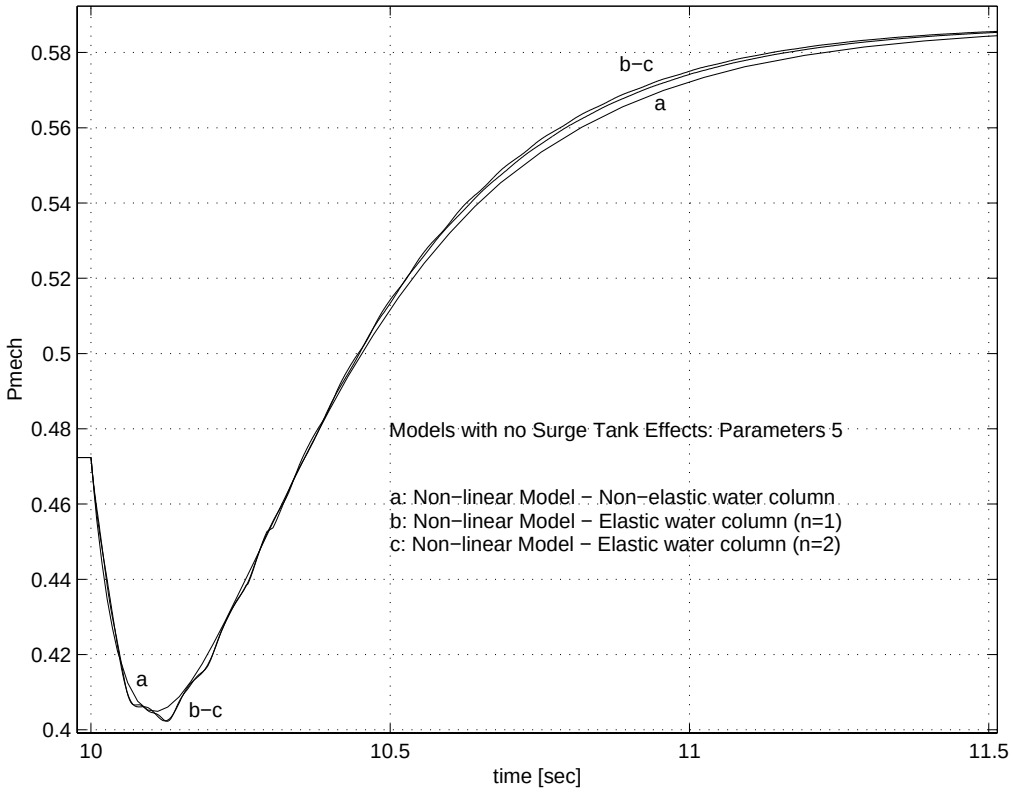

Figure 3.19: Comparison among the models K2, K31 and K32.

Once again, in these models one can observe the phase lag behaviour described in section (3.6.3.1).

3.6.4 Linearized Models with no Surge Tank Effects

These models are based on schemes given by equation (3. 42). Since these models are linearized at an operating point, it is necessary to use $T_{\overline{w}}$, which is calculated using equation (3. 63).

3.6.4.1 Model K_{lin}

The dynamic response of this model is simulated by using the parameters from the following plants: G-Gilboa 3, St. Lawrence 32 and Niagara 1 (Table 3.5). In Figure 3.20 different characteristics can be observed when the gate opening varies by a one per cent according to a step function (0.01 per units). In order to compare the different responses, the steady state of the mechanical power has been forced to be the same for the three power plants by using the same value of the penstock head loss coefficient (f_{p1}).

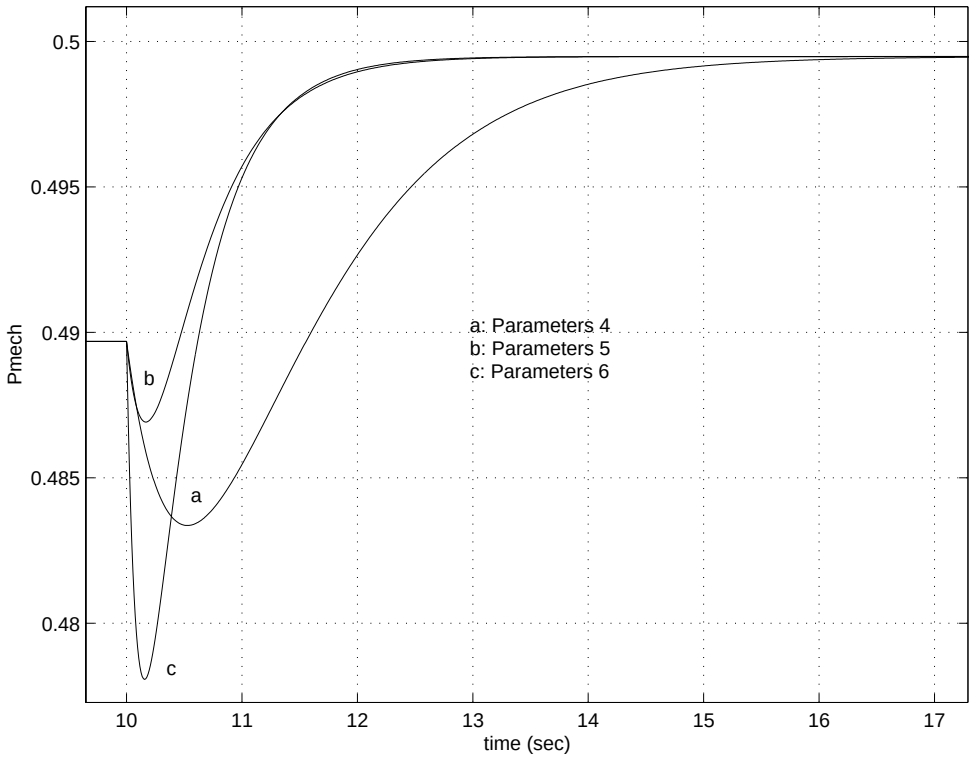

Figure 3.20: Simulation of the model K_{lin} (n=0) by using the parameters of G-Gilboa 3, St. Lawrence 32 and Niagara 1.

Figure 3.20 shows the way the behaviour of a hydroelectric model with no surge tank effects varies during the transient, for different parameters T_{ep}, T_{WP} and A_t.

3.6.4.2 Classic linear model with ideal turbine (Gaden, 1945) - Model G_{lin0}

In this model the friction or head loss coefficients of the penstock are not considered, and the value of the steady sate is uniquely determined by the gate opening $\overline{G}$.

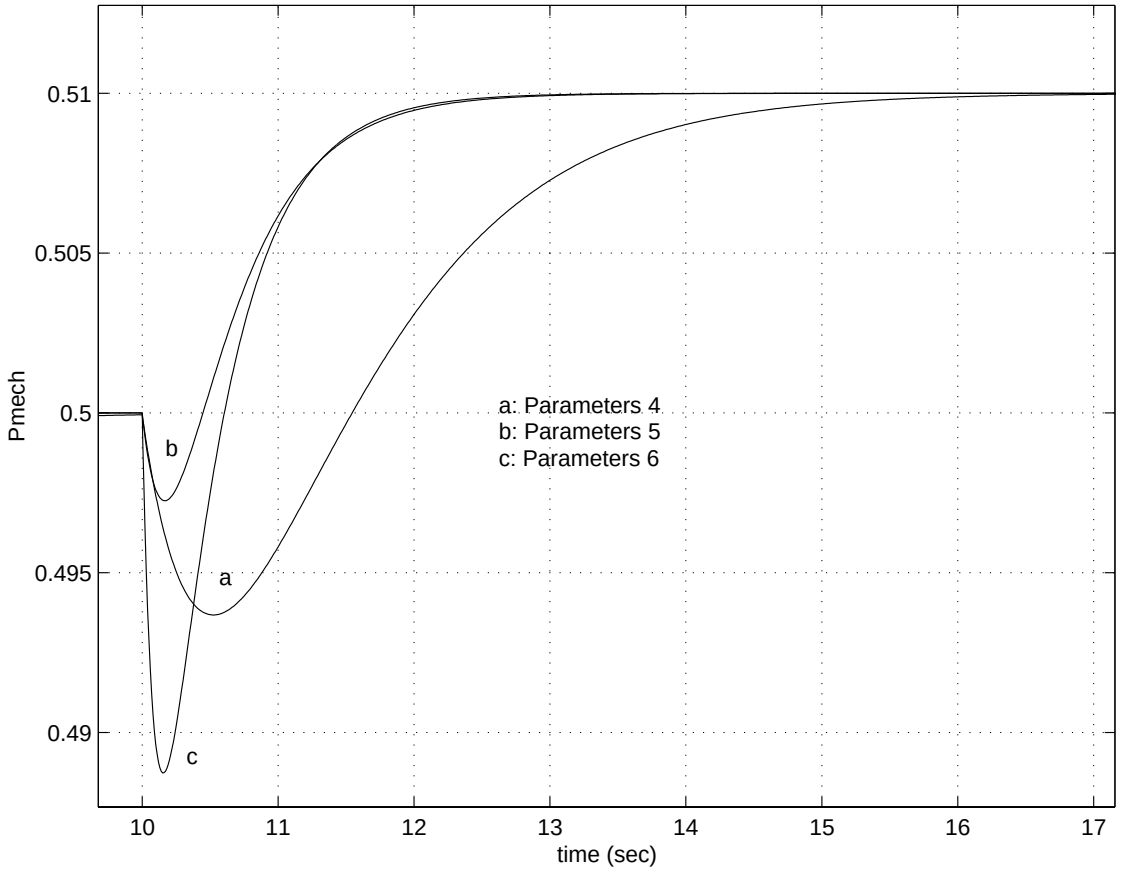

Figure 3.21: Simulation of the classic linear model G_{lin0}.

Figure 3.21 represents the way the parameters T_{ep}, T_{WP} and A_t affect the behaviour of the hydroelectric plant with no surge tank effects during the transient.

3.6.5 Conclusions of the Time Domain Analysis

From the time domain analysis some interesting conclusions can be deduced, they are enumerated below:

- In Figures 3.10 and 3.13 the responses of the models WG4 and K4 present a phase lag in the transient that is not observed in models with similar characteristics but without surge tank effects. This fact can be checked in Figures 3.18 and 3.19, where the response after

applying a step function of a ten per cent on the gate opening of the models (WG2, QR31, QR32, QR33, WG3; and K2, K31, K32) are depicted. This phenomenon is due to the parameter T_{ep}, whose value for the model without a surge tank is up to a magnitude order less than the case of a model with a surge tank, as Table 3.5 shows, i.e. T_{ep} = 0.208 s (Susqueda, with a surge tank) and T_{ep} = 0.0205 s (St. Lawrence 32, without a surge tank).

- In Figure 3.10, moreover, it can be seen that the models QR51 and QR52, where the approximations of the hyperbolic tangent are n=1 and n=2 respectively, have a great similarity respect to the model WG5. This similarity is improved by taking larger values of n in the approximation.

- After the transient, the models WG5, QR52, QR51, WG4, K52, K51 and K4 have the same response. This means that there appears a damped oscillation whose period is given by T. This behaviour is shown in Figures 3.11 and 3.14.

- Another way to verify that the supposition made in Subsection 3.5.1.4, ($f_{p1} = \Phi_p$ and $f_{p2} = \Phi_c$) is correct, it is by means of the similarities among the responses of the models of WG4, QR51 and QR52 (graphics a, b and c, respectively, in Figure 3.10), with respect to the models K4, K51 and K52 presented in Figure 3.13.

- The models WG3, QR33, QR32, QR31, WG2, K32, K31 and K2, as Figures 3.18 and 3.19 show, have similar behaviours since there is not phase lag during the transient.

- In the case of linearized models with surge tank effects, only Q_{lin0} is considered since the models Q_{lin1} and Q_{lin2}, with approximations of the hyperbolic tangent greater than n=0, are unstable, as is it shown in Section 3.7.

- Linearized models without surge tank effects (K_{lin} and G_{lin0}) have a particular interest since they allow to observe the variations that appear during non-minimal phase behaviour, which, in essence, are due to differences among parameters T_{WP} and T_{ep}.

3.7 Frequency Response Analysis of Models

In this Section is presented an analysis of the linearized models described in Section 3.3. The parameters of Table 3.5 are also utilised for this study. For an easier understanding of this study, the different analyses are separated into two sections. Each section presents the frequency responses, Bode plots and the Nyquist diagrams, where the stability is verified. The sections are:

- Section 3.7.1, where the behaviours of the models K_{lin} and G_{lin0} *without* surge tank effects are presented.
- Section 3.7.2, where the behaviours of the models Q_{lin} and Q_{lin0} *with* surge tank effects are presented.

Moreover, it is important to mention that Oldenburger and Donelson (1962) present a complete frequency response study of linearized models for different working points. In this Section the analysis for the linearized models working at an operating point is presented in order to illustrate the behaviour of them in a certain situation.

3.7.1 Models with no Surge Tank Effects

3.7.1.1 Models K_{lin} and G_{lin0}

The point of departure is equation (3. 42) that represents the relationship between the mechanical power and the gate opening. In Figure 3.22 is depicted a Bode plot for the linearized model without surge tank for the approximations n=0,1 of the hyperbolic tangent.

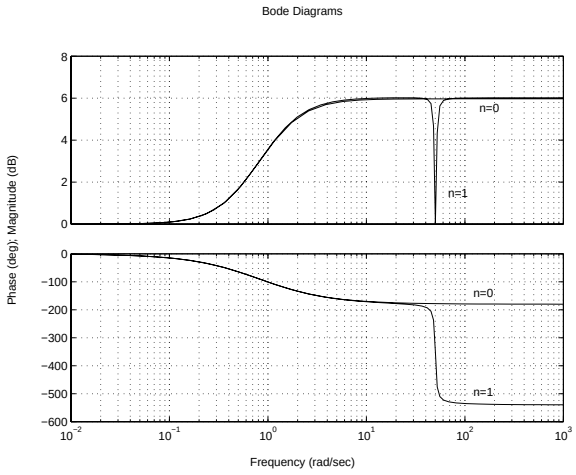

Figure 3.22: Bode plot for models of K_{lin}, approximations n = 0, 1. Parameters B. Gilboa 3.

In Figures 3.22, 3.23 and 3.24 the parameters from B. Gilboa 3 (a hydroelectric plant without a surge tank Table 3.5) are used.

3.7.1.2 Stability Study

In Figures 3.23 and 3.24 Nyquist diagrams for models K_{lin} with n = 0, 1 are presented. In both cases the point (-1,0) of the complex plane is rounded in the clockwise sense, which, for a non-minimal phase transfer function, means that this is a stable system.

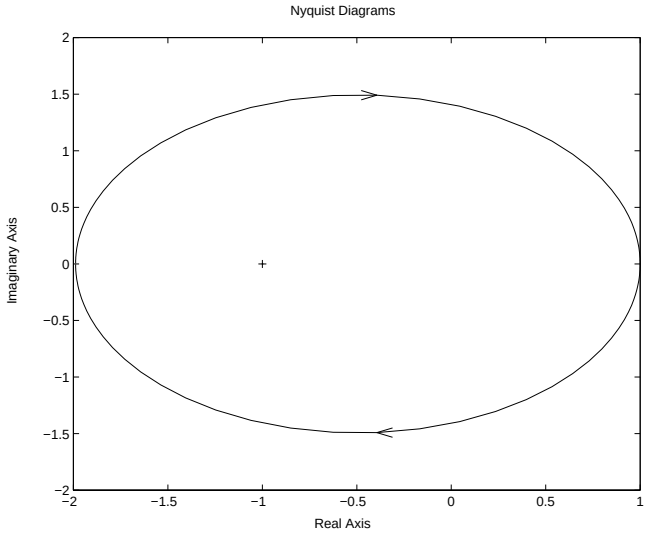

Figure 3.23: Nyquist diagram for the model of G_{lin0}, approximation n = 0. Parameters from B. Gilboa 3.

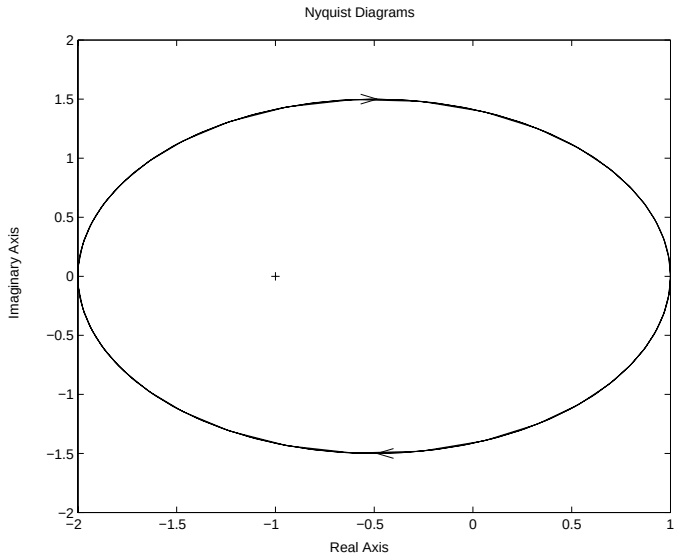

Figure 3.24: Nyquist diagram for the model of K_{lin}, approximation n = 1. Parameters from B. Gilboa 3.

3.7.2 Models with Surge Tank Effects

3.7.2.1 Models Q_{lin} and Q_{lin0}

The Bode plots are obtained by using the equation (3. 41) when is considered non-elastic water columns, and equation (3. 40) when an elastic water column in the penstock and non-a elastic water column in the tunnel are considered.

In Figure 3.25 the Bode plot for the model with the approximation of n=0 is shown. The models with the lumped parameter approximations, n=1,2, represent unstable transfer functions, as can be seen in Figures 3.29 and 3.31.

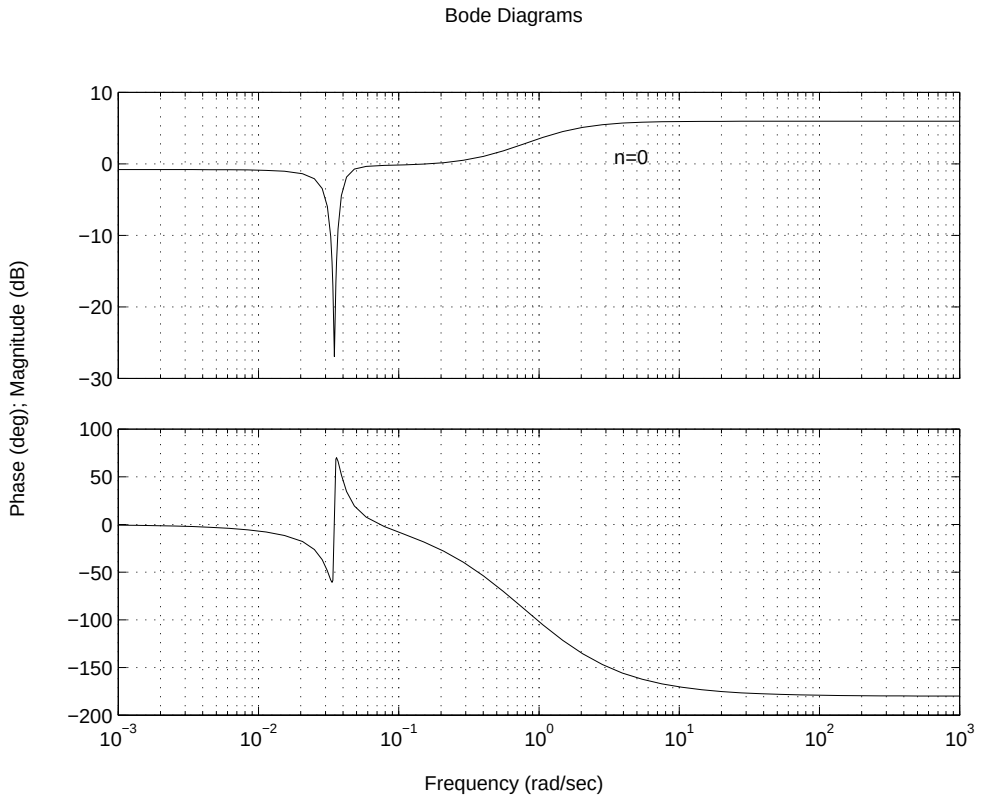

Figure 3.25: Bode plot for the model of Q_{lin0}, approximation n = 0. Parameters from (IEEE Working Group, 1992).

Figures 3.25 to 3.32 consider the parameters of the hydroelectric plants of IEEE Working Group and Appalachia (Table 3.5). The reason of considering two power plants is mainly to verify whether the model Q_{lin} for the approximations n=1,2 is stable or not.

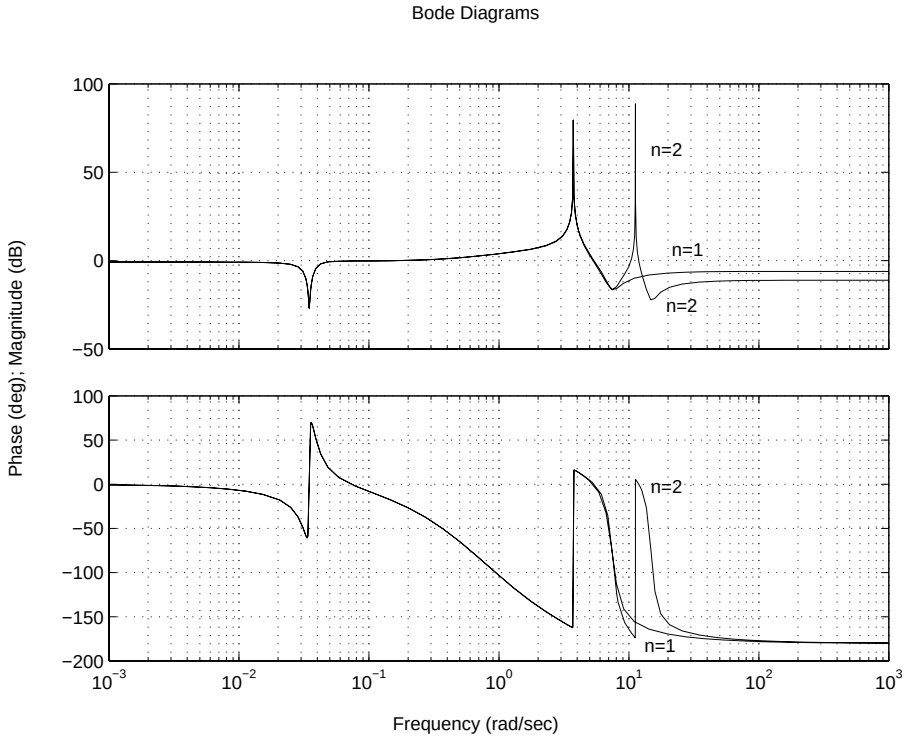

Figure 3.26: Bode plot for the model of Q_{lin}, approximations n = 1, 2. Parameters from (IEEE Working Group, 1992).

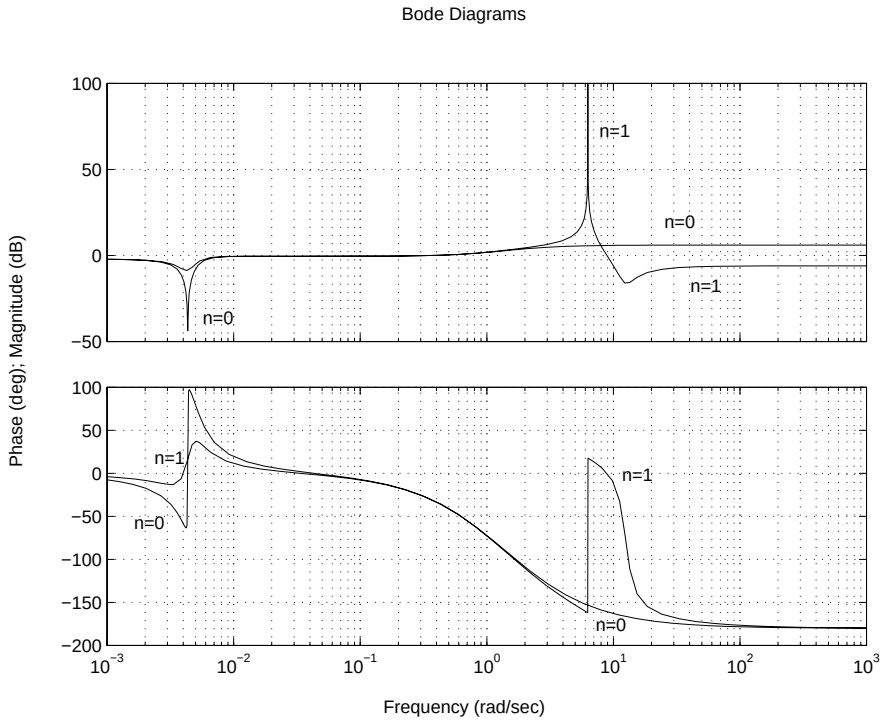

Figure 3.27: Bode plot for the model of Q_{lin0} and Q_{lin}, approximations n = 0, 1. Parameters from Appalachia power plant.

3.7.2.2 Stability Study

The Nyquist diagram shows that the model of Q_{lin}, where non-elastic water columns (n=0) are considered, is stable since the diagram rounds the point of the complex plane (-1,0) in a clockwise sense. This can be verified in Figure 3.28.

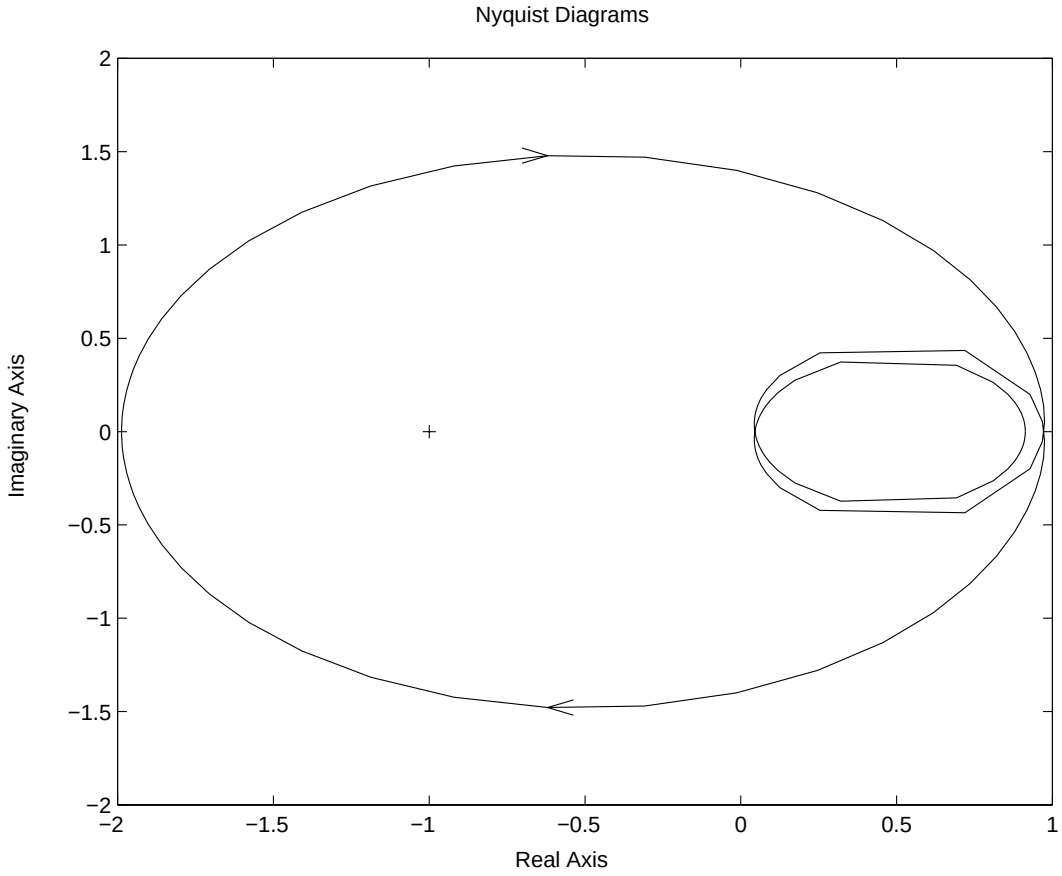

Figure 3.28: Nyquist diagram for the model Q_{lin}, approximation n = 0. Parameters from (IEEE Working Group, 1992).

When the lumped approximations (n=1,2) of the model Q_{lin} are considered, the system becomes unstable since the Nyquist diagram does not round the point (-1,0) in the clockwise sense, which for a non-minimal phase system means instability. This fact is shown in Figures 3.29 and 3.30.

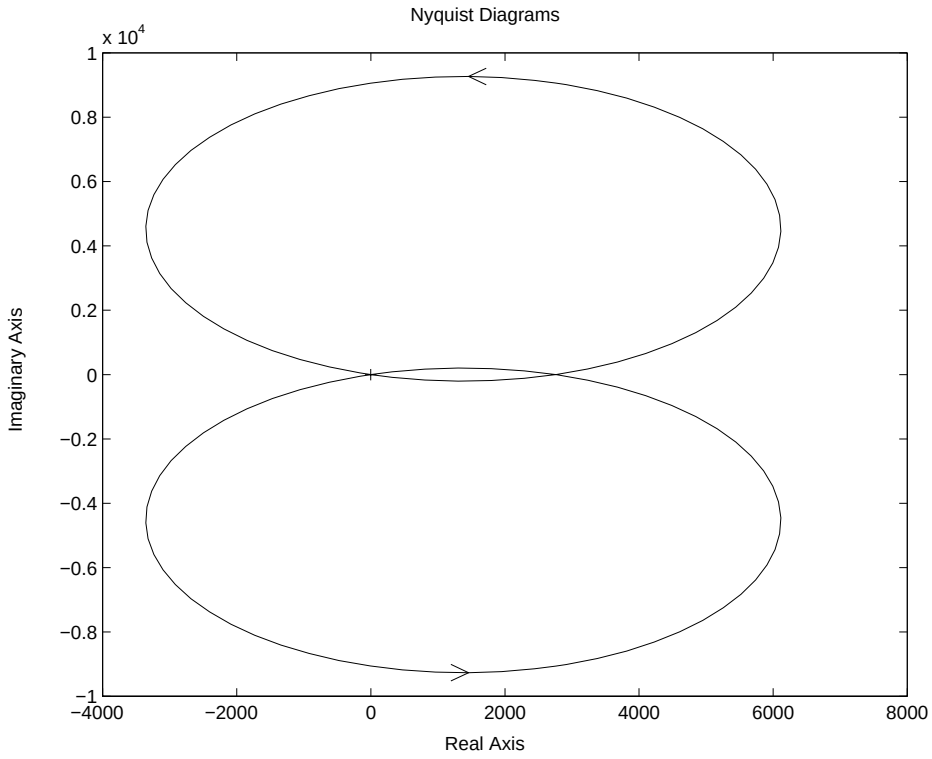

Figure 3.29: Nyquist diagram for the model of Q_{lin}, approximation n = 1. Parameters from (IEEE Working Group, 1992).

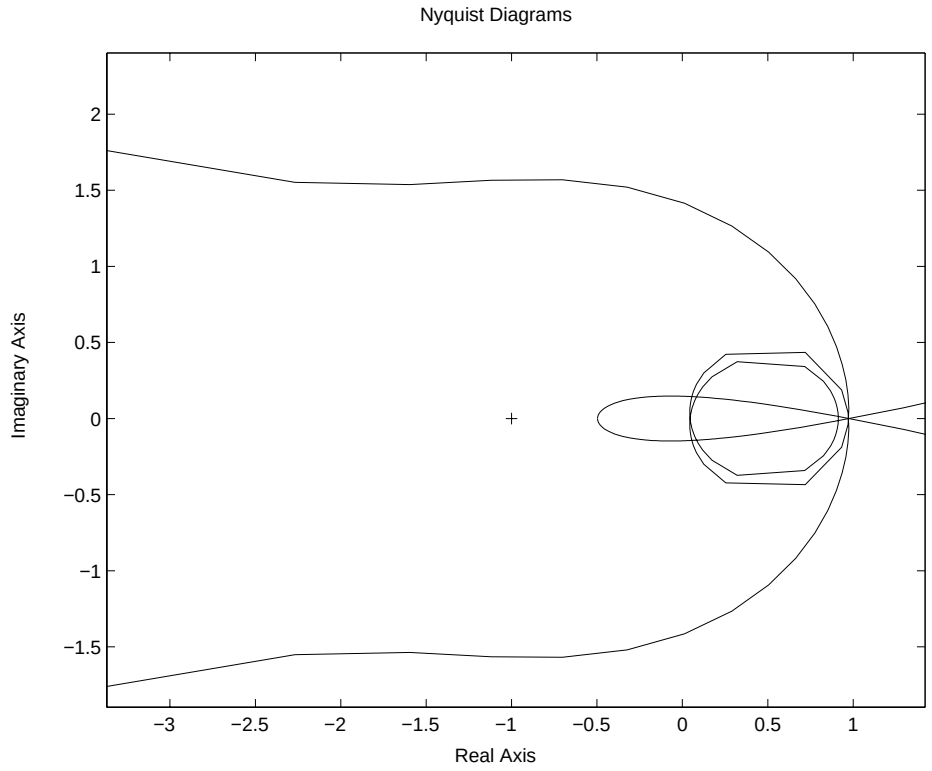

Figure 3.30: Detail of Figure 3.29.

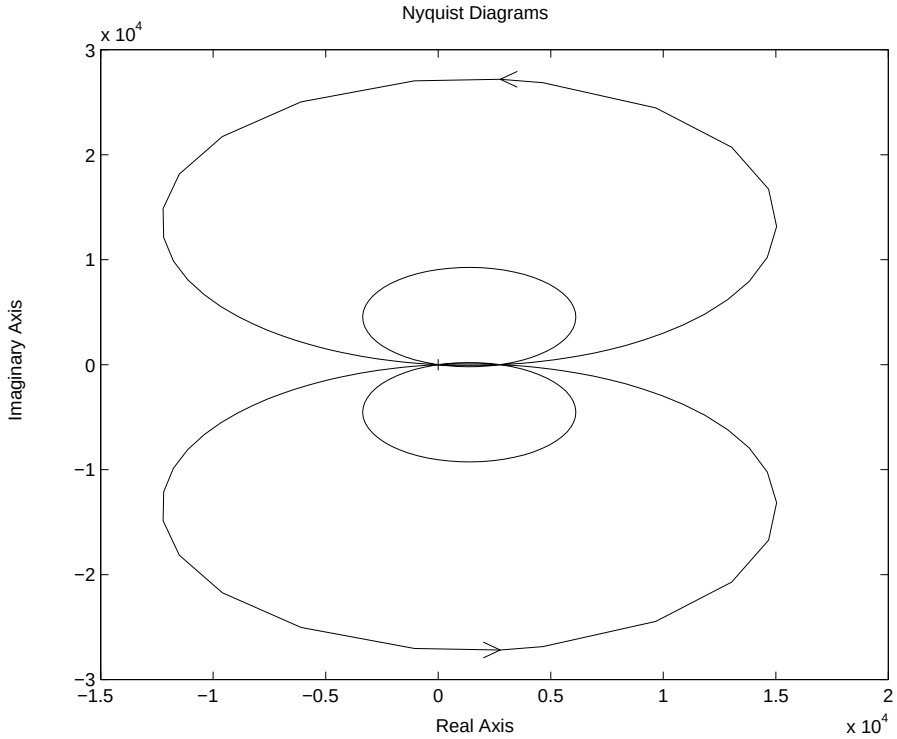

Figure 3.31: Nyquist diagram for the model Q_{lin}, approximation n = 2. Parameters from (IEEE Working Group, 1992).

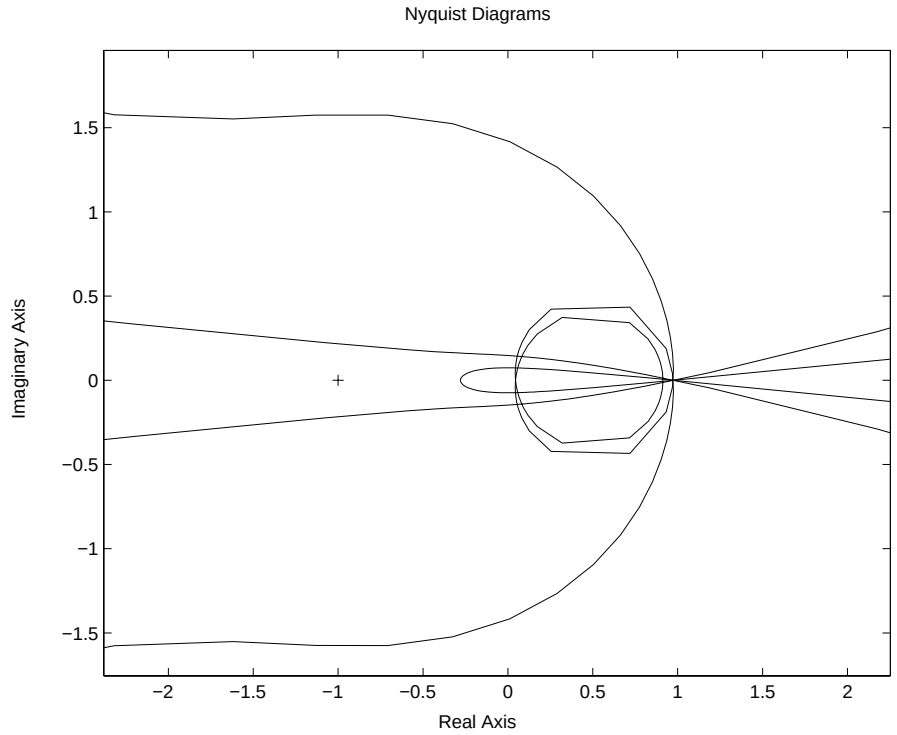

Figure 3.32: Detail of Figure 3.31.

3.8 Suggestions for Modelling Hydroelectric Power Plants

After presenting the time domain and frequency response analyses of different models for hydroelectric power plants, some suggestions are given below that add more information to the *Guidelines for Modelling Hydraulic Turbines* presented in Section 9.1.5 of Kundur (1994). These complementary suggestions are divided into two parts, on one hand the hydroelectric models that consider surge tank effects, and, on the other hand, the hydroelectric models without surge tank effects.

3.8.1 Models with Surge Tank Effects

3.8.1.1 Nonlinear Models

For this case some models deduced according to two different ways are presented:

1) The model WG5 allows the best approximation since it represents all the phenomena in detail. On one hand, the model WG5 shows the non-minimal-phase behaviour for a step input. On the other hand, the model WG5 has the inconvenient of incorporating the hyperbolic tangent function of complex variable in an equation system of state variables. Therefore, when a control must be designed, instead of WG5, it is necessary to take the lumped approximations of this function and the model WG5 is turned into QR52, QR51 or WG4.

The greater the value of the lumped approximation, the greater the number of state variables. In the case of working with an interconnected system, it is probable that the models WG4 and QR51 are sufficient to represent, in a very accurate manner, the behaviour of a hydroelectric plant with surge tank effects.

2) The models of Kundur (1994) K5, K52 and K51 have the disadvantage that the variable $\overline{U}_0$ must be updated for each value of the gate opening ($\overline{G}$). Apart from this, the models of Kundur (1994) have similar behaviours with respect to the models WG5, QR52 and QR51. For these reasons the models of Kundur are interesting in the analysis of the hydroelectric plant in a general sense but not for the design of a speed system control.

3.8.1.2 Linearized Models

These models are interesting when a frequency response study is necessary for stability studies. However, only the simplest model can be used since these models are unstable for lumped approximations greater than n=0.

3.8.2 Models with no Surge Tank Effects

3.8.2.1 Nonlinear Models

In this case there appears a similar situation to the case of nonlinear models with surge tank effects: the model that considers the hyperbolic tangent function, calculated according to Figure 3.18, gives the best approximation to the real system, and there is only a slight difference among the four lumped approximations n=0,1,2,3 and the model that takes the complete hyperbolic tangent (WG3).

For the K3, K32 and K32 models the conclusions exposed for hydroelectric plants with surge tank effects are still valid. Therefore, these models are interesting for performing behaviour analysis and *not* for designing controllers.

3.8.2.2 Linearized Models

The models K_{lin} and G_{lin} are useful in those cases when small-signal stability studies are required (Kundur, 1994).

3.9 Summary

A study of hydroelectric models has been presented in this Chapter. This study classifies the models into two groups: *nonlinear models and linearized models*, Sections 3.2 and 3.3, respectively. Each group has been subdivided into *models with and without surge tank effects*. Moreover, each of these has two particularities: *the first considers elastic water column in the penstock and non-elastic water column in the tunnel, and the second contemplates non-elastic water columns*. In the group of nonlinear models, with or without surge tank effects, a comparison has been performed where differences and similarities among the models are shown.

Subsequently, Section 3.5, presented a way to calculate the turbine and tunnel flows in steady state, which allows to calculate the mechanical power in steady state as function of the gate opening.

Section 3.6 presented a time domain analysis where all models have been simulated for different real hydroelectric plants (parameters are shown in Table 3.5). The behaviours have been compared.

All linearized models have been used in the frequency response analysis, which is exposed in Section 3.7. Bode plots and Nyquist diagrams have been presented for the determination of the stability of these models.

In Section 3.8 suggestions for modelling hydroelectric plants are proposed.